

## **Towards Enhancing Spin States in Doped Arylamine Compounds through Extended Planarity of the Spin Coupling Moieties**

Łukasz Skórka,<sup>[a]</sup> Jean-Marie Mouesca,<sup>[b],[c]</sup> Jacek B. Gosk,<sup>[d]</sup> Roman Puźniak,<sup>[e]</sup>  
Jacques Pécaut,<sup>[b],[c]</sup> Vincent Maurel\*<sup>[b],[c]</sup> and Irena Kulszewicz-Bajer\*<sup>[a]</sup>

*<sup>a</sup> Faculty of Chemistry, Warsaw University of Technology, noakowskiego 3, 00-664 Warsaw, Poland*

*<sup>b</sup> INAC, SyMMES Université Grenoble Alpes, F-38000 Grenoble, France*

*<sup>c</sup> INAC, SyMMES, CEA Grenoble, F-38054 Grenoble, France*

*<sup>d</sup> Faculty of Physics, Warsaw University of Technology, Koszykowa 75, 00-662 Warsaw, Poland*

*<sup>e</sup> Institute of Physics, Polish Academy of Science, Al. Lotników 32/46, 02-668 Warsaw, Poland*

## Electronic Supplementary Information

### Content

3

II.	Synthetic procedures.....	S3
III.	Crystallographic Data .....	S32
IV.	Oxidation Procedure for Pulsed EPR and SQUID Experiments .....	S34
V.	The electrochemical oxidation of QA, PQA, D2 and PA2 (CV curves).....	S34
VI.	UV-vis-NIR spectra of QA and PQA recorded during chemical oxidation. ....	S36
VII.	Pulsed EPR Nutation Measurements by PEANUT Experiment.....	S37
VIII.	SQUID Magnetometry.....	S39
IX.	DFT Methodology .....	S48
X.	References.....	S52

## I. General Information

### *General Reagent Information*

2,6-diaminotoluene, 1-hexyne, 1-bromohexane, ethynyltrimethylsilane, 4-iodoanisole, 4-iodophenol, 4-hexyloxyaniline, 4-methoxyaniline (*p*-anisidine), 4-bromoanisole, bromobenzene, potassium carbonate, methyltriphenylphosphonium bromide, *n*-butyllithium solution, 2-bromobenzoic acid, methylmagnesium chloride solution, phosphoric acid, ammonium formate, palladium on activated charcoal 10% Pd/C, tris(4-bromophenyl)amminium hexachloroantimonate TBA\*SbCl<sub>6</sub>, copper(I) iodide CuI, palladium acetate Pd(OAc)<sub>2</sub>, tris(dibenzylideneacetone)dipalladium(0) Pd<sub>2</sub>dba<sub>3</sub>, tri-*tert*-butylphosphine *t*-Bu<sub>3</sub>P, 2,2'-bis(diphenylphosphino)-1,1'-binaphtyl BINAP, sodium *tert*-butoxide *t*-BuONa, NBS, triethylamine, anhydrous solvents (packed in Sure-Seal bottles): toluene, dichloromethane, acetonitrile, THF, DMF and 1,4-dioxane were purchased from Sigma Aldrich Co. 2-bromiodobenzene, benzaldehyde, sodium cyanoborohydride NaBH<sub>3</sub>(CN) were purchased from Alfa Aesar. Concentrated sulfuric acid, magnesium sulfate, sodium sulfate, acetic anhydride, acetic acid, hexane, dichloromethane, THF, ethyl acetate, methanol and ethanol were obtained from POCH or other local suppliers. Dichlorobis(triphenylphosphine)palladium(II)<sup>1</sup> was synthesized according to literature procedure. 2,6-diaminotoluene was further purified prior to use by column chromatography (in ethyl acetate) and stored under argon atmosphere. 4-methoxyaniline was recrystallized from water/ethanol prior to use. The remaining chemicals were used as received. All glassware was oven-dried, assembled hot, and cooled under a dry argon stream before use. Unless stated otherwise, all reactions were performed under the flow of dry argon.

### *Characterization Techniques Information*

All new compounds were characterized by NMR spectroscopy, IR spectroscopy and elemental analysis. Additionally, the final compounds were characterized using mass spectrometry and high-resolution mass spectrometry. In one case, the structure and absolute configurations were also determined with the aid of X-ray study on a single crystal.

<sup>1</sup>H and <sup>13</sup>C NMR spectra were recorded on one of the following spectrometers: Varian Mercury 400 MHz, Varian VNMRs 600 MHz, Varian NMR System 500 MHz or Bruker

AVANCE III 500 MHz.  $^1\text{H}$  NMR data were reported as follows: chemical shift in reference to residual solvent peak - 29.84 ppm for acetone- $d_6$ ,<sup>2</sup> 128.06 ppm for  $\text{C}_6\text{D}_6$ ,<sup>2</sup> 77.16 ppm for  $\text{CDCl}_3$ ,<sup>2</sup> 39.52 ppm for DMSO- $d_6$ <sup>2</sup> and 67.21 ppm for THF- $d_8$ <sup>2</sup> ( $\delta$  ppm), multiplicity (s = singlet, d = doublet, q = quartet, dd = doublet of doublets, ddd = doublet of doublets of doublets, td = triplet of doublets, m = multiplet), coupling constant (Hz), integration.  $^{13}\text{C}$  NMR data were reported as chemical shifts ( $\delta$  ppm) referenced to residual solvent peak: 2.05 ppm for acetone- $d_6$ ,<sup>2</sup> 7.16 ppm for  $\text{C}_6\text{D}_6$ ,<sup>2</sup> 7.26 ppm for  $\text{CDCl}_3$ ,<sup>2</sup> 2.50 ppm for DMSO- $d_6$ <sup>2</sup> and 3.58 ppm for THF- $d_8$ <sup>2</sup>.

IR spectra were monitored on one of the following devices: FT-IR Paragon 1000 spectrometer (ATR), Nicolet iS5 Thermo Scientific spectrometer (ATR) as liquids or solids or on BIO-RAD FPS-165 FT-IR spectrometer (KBr pallets). Data was reported as absorption *versus* reciprocal centimeters ( $\text{cm}^{-1}$ ).

Elemental analysis was carried out on CHNS analyzer (model Vario EL III) manufactured by Elementar Analysensysteme GmbH.

Mass Spectra were recorded on magnetic sector mass spectrometer *AutoSpec Premier* (Waters, USA), equipped with an electron impact (EI) ion source and the EBE double focusing geometry mass analyzer or MALDISynapt G2-S HDMS (Waters Inc) mass spectrometer equipped with an electrospray ion source and q-TOF type mass analyzer or Mariner PE Biosystems. The instruments were controlled and recorded data were processed using *MassLynx V4.1* software package (Waters Inc).

Diffraction data were collected using an Oxford Diffraction XCallibur S Kappa area detector four-circle diffractometer (Mo-K $\alpha$  radiation  $\lambda = 0.71073 \text{ \AA}$ , graphite monochromator), controlled by the Oxford Diffraction CrysAlis CCD software.<sup>3</sup> Unique intensities with  $I > 10\sigma(I)$  detected on all frames using the Oxford Diffraction RED were used to refine the values of the cell parameters. The substantial redundancy in data allowed analytical absorption corrections to be applied using crystal shape determination. The space group was determined from systematic absences, and it was confirmed by the successful resolution of the structure. The structure was solved by direct method using ShelxT<sup>4</sup> software in Olex2.1<sup>5</sup> environment and all the atoms were found by difference Fourier syntheses. All non-hydrogen atoms were anisotropically refined on  $F^2$  using ShelXL program<sup>4</sup> while hydrogen atoms were isotropically refined (X-ray data can be obtained free of charge from the Crystallographic Data Centre via [www.ccdc.cam.ac.uk/data\\_request/cif](http://www.ccdc.cam.ac.uk/data_request/cif). CCDC numbers xxx).

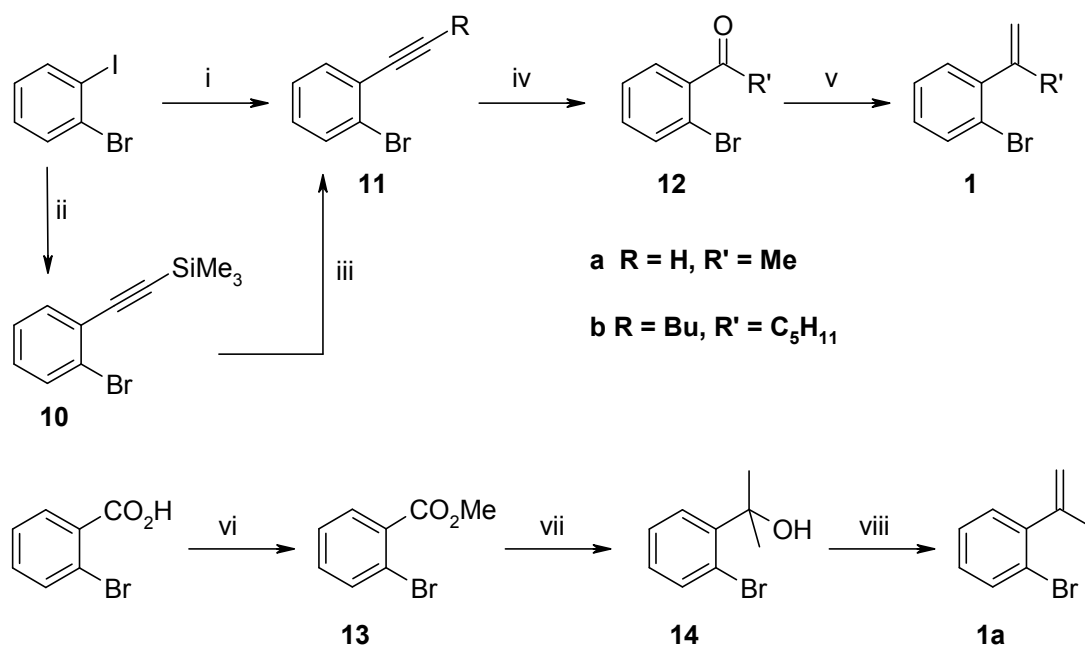
Gel permeation chromatography was performed on GPCMax TDA 305 manufactured by Malvern Instruments Ltd., using JORDI LABS Mixed Bed column and refractometer as a detector. The experiment was performed at 30 °C with 1 mL per minute dichloromethane flow and calibrated for polystyrene standard.

UV-Vis-NIR spectra were recorded using a Cary 5000 (Varian) spectrometer in quartz cuvettes with optical path length 0.1 mm or 1.0 mm.

The electrochemical oxidation was monitored by cyclic voltammetry. For these investigations the compounds were dissolved in CH<sub>2</sub>Cl<sub>2</sub> (1 x 10<sup>-3</sup> M). The experiments were carried out in a one compartment electrochemical cell, in a solution of 0.1 M Bu<sub>4</sub>NBF<sub>4</sub> in CH<sub>2</sub>Cl<sub>2</sub> with Ag/0.1 M AgNO<sub>3</sub> in acetonitrile as a reference electrode and a Pt counter electrode. Scan rate was 100mV/s. The surface of Pt disk electrode was 3 mm<sup>2</sup>. The potential of Fc/Fc<sup>+</sup> = 0.155 V vs. Ag/Ag<sup>+</sup> in cyclic voltammetry of D2, PA2 and PQA and 0.173 V for QA voltammetry.

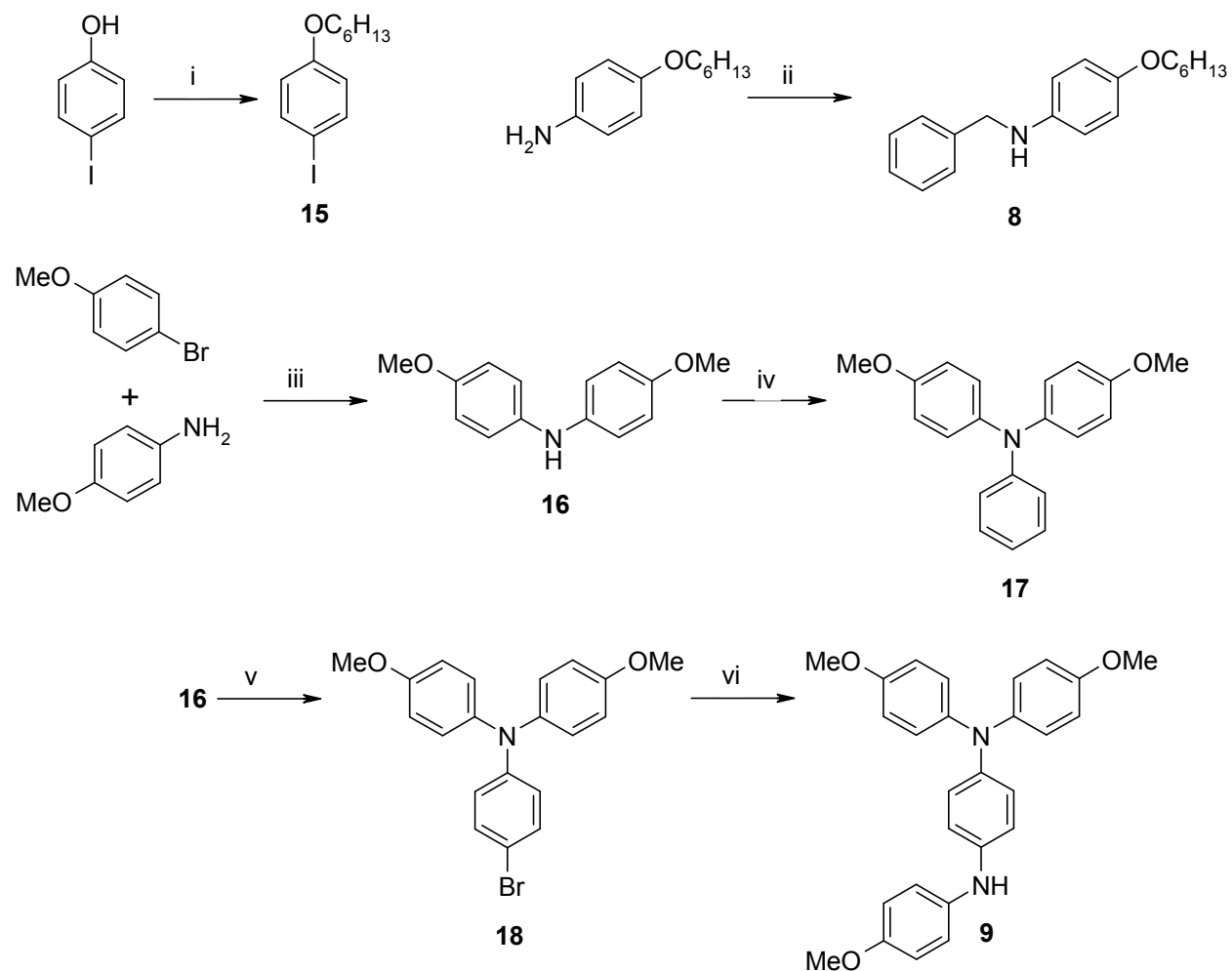
## II. Synthetic procedures

**Scheme S1.** Synthesis of intermediate bromides 1a and 1b

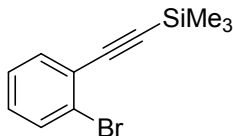


**Conditions:** (i) 1-hexyne, 5% [PdCl<sub>2</sub>(PPh<sub>3</sub>)<sub>2</sub>], 10% CuI, NEt<sub>3</sub>, THF, Ar, rt (ii) ethynyltrimethylsilane, 5% [PdCl<sub>2</sub>(PPh<sub>3</sub>)<sub>2</sub>], 10% CuI, NEt<sub>3</sub>, rt (iii) K<sub>2</sub>CO<sub>3</sub>, MeOH/THF, Ar, rt (iv) HCO<sub>2</sub>H, Ar, 100 °C (v) 1. CH<sub>3</sub>PPh<sub>3</sub>Br, BuLi, THF, Ar, 0 °C (vi) H<sub>2</sub>SO<sub>4</sub>, MeOH, reflux (vii) MeMgCl, THF, Ar, 0 °C (viii) H<sub>2</sub>SO<sub>4</sub>, MeCO<sub>2</sub>H, Ac<sub>2</sub>O, rt

**Scheme S2.** Synthesis of intermediate amines

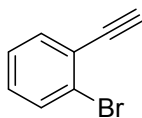


**Conditions:** (i) bromohexane,  $K_2CO_3$ , acetone, reflux (ii) 1. benzaldehyde, MeOH, Ar, rt 2.  $NaBH_3CN$ ,  $MeCO_2H$ . (iii) 3%  $[Pd(OAc)_2]$ , BINAP, *t*-BuONa, toluene, Ar, 110 °C (iv) bromobenzene, 3%  $[Pd(OAc)_2]$ ,  $P(t-Bu)_3$ , *t*-BuONa, toluene, Ar, 110 °C (v) NBS, DMF, Ar, 110 °C (vi) 4-methoxyaniline 3%  $[Pd(OAc)_2]$ , BINAP, *t*-BuONa, toluene, Ar, 110 °C



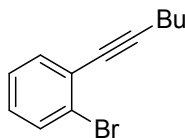
**((2-bromophenyl)ethynyl)trimethylsilane (10)** 2-bromoiodobenzene (44.00 mmol, 13.00 g, 1.00 eq.) and trimethylethynylsilane (55.20 mmol, 5.42 g, 1.20 eq.) were mixed in triethylamine (60 mL) under argon. Then dichlorobis(triphenylphosphine)palladium(II) (2.30 mmol, 1.61 g, 5% mol) and copper(I) iodide (9.20 mmol, 1.75 g, 20% mol) were introduced and the reaction mixture was left with stirring overnight under argon. Then it was extracted with chloroform, dried over magnesium sulfate and evaporated. The crude product was chromatographed with hexane yielding the title product as pale yellow oil. 10.98 g yield: 99%.

$^1\text{H NMR}$  (400 MHz,  $\text{CDCl}_3$ )  $\delta$  7.57 (ddd,  $J = 8.0, 1.3, 0.4$  Hz, 1H), 7.49 (ddd,  $J = 7.7, 1.8, 0.4$  Hz, 1H), 7.24 (ddd,  $J = 7.7, 7.5, 1.3$  Hz, 1H), 7.15 (ddd,  $J = 8.0, 7.5, 1.8$  Hz, 1H), 0.28 (s, 9H).  $^{13}\text{C NMR}$  (100 MHz,  $\text{CDCl}_3$ )  $\delta$  133.71, 132.47, 129.67, 127.00, 125.89, 125.37, 103.15, 99.77, 0.03. **IR** (KBr,  $\text{cm}^{-1}$ ) 3068, 2961, 2899, 2164, 2068, 1586, 1558, 1466, 1435, 1424, 1408, 1251, 1221, 1120, 1046, 1028, 945, 866, 844, 754, 711, 701, 671, 641, 549, 448.



**1-bromo-2-ethynylbenzene (11a)** ((2-bromophenyl)ethynyl)trimethylsilane (1.80 mmol, 0.46 g, 1.00 eq.) and potassium carbonate (0.18 mmol, 25 mg, 0.10 eq.) were added to methanol/THF mixture (5 mL, 1/1) and left stirring overnight. Then it was extracted with chloroform and dried over magnesium sulfate. Upon evaporation of the solvent the title product was obtained as pale yellow oil. 0.29 g yield: 89%.

$^1\text{H NMR}$  (400 MHz,  $\text{CDCl}_3$ )  $\delta$  7.59 (dd,  $J = 8.0, 1.3$  Hz, 1H), 7.53 (dd,  $J = 7.6, 1.8$  Hz, 1H), 7.27 (td,  $J = 7.6, 1.3$  Hz, 1H), 7.20 (td,  $J = 7.7, 1.8$  Hz, 1H), 3.38 (s, 1H).  $^{13}\text{C NMR}$  (100 MHz,  $\text{CDCl}_3$ )  $\delta$  134.21, 132.57, 130.10, 127.12, 125.68, 124.39, 81.94. **IR** (KBr,  $\text{cm}^{-1}$ ) 3293, 3067, 2367, 2358, 2342, 2327, 2113, 1958, 1927, 1708, 1589, 1559, 1466, 1435, 1424, 1257, 1165, 1120, 1045, 1027, 947, 773, 754, 661, 628, 540, 446.



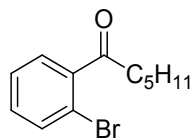
**1-bromo-2-(hex-1-yn-1-yl)benzene (11b)** The same procedure as for ((2-bromophenyl)ethynyl)trimethylsilane incorporating 2-bromoiodobenzene (20.00 mmol, 5.66 g, 1.00 eq.), 1-hexyne (24.00 mmol, 1.97 g, 1.20 eq.), dichlorobis(triphenylphosphine)palladium(II) (1.00 mmol, 0.70 g, 0.05 eq.), copper(I) iodide (2.00 mmol, 0.38 g, 0.10 eq) and a mixture of triethylamine (10 mL) with anhydrous THF (20 mL) afforded the title compound as pale yellow oil. 4.54 g yield: 96%

**<sup>1</sup>H NMR** (400 MHz, CDCl<sub>3</sub>) δ 7.55 (dd, *J* = 8.0, 1.3 Hz, 1H), 7.42 (dd, *J* = 7.6, 1.7 Hz, 1H), 7.22 (td, *J* = 7.6, 1.3 Hz, 1H), 7.11 (ddd, *J* = 8.0, 7.6, 1.7 Hz, 1H), 2.47 (t, *J* = 6.9 Hz, 2H), 1.68 – 1.56 (m, 2H), 1.57 – 1.46 (m, 2H), 0.96 (t, *J* = 7.2 Hz, 3H). **<sup>13</sup>C NMR** (100 MHz, CDCl<sub>3</sub>) δ 133.39, 132.35, 128.73, 126.98, 126.15, 125.55, 95.67, 79.42, 30.77, 22.12, 19.42, 13.81. **IR** (cm<sup>-1</sup>) 3061, 2956, 2929, 2872, 2207, 1588, 1468, 1433, 751. **Anal. Calcd. for** C<sub>12</sub>H<sub>13</sub>Br: C, 60.78; H, 5.53; Br, 33.70. Found: C, 60.88; H, 5.83.



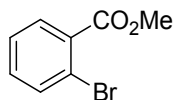
**1-(2-bromophenyl)ethanone (12a)** 1-bromo-2-ethynylbenzene (30.30 mmol, 5.49 g) in formic acid (70 mL) was heated to 100 °C under argon for 4 hours. Then it was neutralized with saturated potassium carbonate solution and extracted with chloroform. Upon drying with magnesium sulfate, the solvent was evaporated and the crude product was chromatographed using hexane/dichloromethane (2/1) solution, which gave the expected product as yellow oil. 5.83 g, yield: 97%.

**<sup>1</sup>H NMR** (400 MHz, CDCl<sub>3</sub>) δ 7.61 (dd, *J* = 7.9, 1.2 Hz, 1H), 7.46 (dd, *J* = 7.6, 1.8 Hz, 1H), 7.37 (td, *J* = 7.5, 1.2 Hz, 1H), 7.29 (ddd, *J* = 7.9, 7.4, 1.8 Hz, 1H), 2.63 (s, 3H). **<sup>13</sup>C NMR** (100 MHz, CDCl<sub>3</sub>) δ 201.45, 141.57, 133.94, 131.89, 129.02, 127.54, 119.01, 30.48. **IR** (KBr, cm<sup>-1</sup>) 3384, 3068, 3008, 2929, 2855, 2361, 2317, 1939, 1701, 1588, 1564, 1466, 1427, 1356, 1284, 1242, 1164, 1127, 1092, 1027, 961, 870, 758, 743, 722, 653, 594, 534, 452.



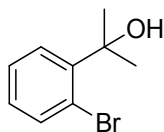
**1-(2-bromophenyl)hexan-1-one (12b)** 1-bromo-2-(hex-1-yn-1-yl)benzene (18.22 mmol, 4.32 g) in formic acid (60 mL) was heated to 100 °C under argon overnight. Then it was neutralized with saturated potassium carbonate solution and extracted with chloroform. Upon drying with magnesium sulfate, the solvent was evaporated and the crude product was chromatographed using hexane/dichloromethane (2/1) solution, which gave the expected product as yellow oil. 3.62 g, yield: 78%.

**<sup>1</sup>H NMR** (400 MHz, CDCl<sub>3</sub>) δ 7.61 – 7.57 (m, 1H), 7.37 – 7.34 (m, 2H), 7.31 – 7.25 (m, 1H), 2.90 (t, *J* = 7.4 Hz, 2H), 1.78 – 1.64 (m, 2H), 1.44 – 1.25 (m, 4H), 0.90 (t, *J* = 7.1 Hz, 3H). **<sup>13</sup>C NMR** (100 MHz, CDCl<sub>3</sub>) δ 204.88, 142.18, 133.69, 131.42, 128.32, 127.48, 118.66, 42.93, 31.48, 23.92, 22.63, 14.11. **IR** (cm<sup>-1</sup>) 3064, 2955, 2928, 2870, 1699, 1587, 1563, 1465, 1428, 1287, 754. **Anal. Calcd. for** C<sub>12</sub>H<sub>15</sub>BrO: C, 56.49; H, 5.93; Br, 31.32; O, 6.27. Found: C, 57.00; H, 6.81.



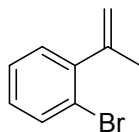
**Methyl 2-bromobenzoate (13)** 2-bromobenzoic acid (30.00 mmol, 6.03 g) was dissolved in 50 mL of methanol. To the solution 1 mL of concentrated sulfuric acid was added and the mixture was heated to reflux for 4 hours. Then it was neutralized with saturated sodium carbonate solution and extracted with ethyl acetate. The organic phase was dried over magnesium sulfate and evaporated to afford the title compound as pale yellow oil. 5.91 g yield: 92%.

**<sup>1</sup>H NMR** (400 MHz, CDCl<sub>3</sub>) δ 7.81 – 7.76 (m, 1H), 7.68 – 7.63 (m, 1H), 7.39 – 7.29 (m, 2H), 3.93 (s, 3H). **IR** (cm<sup>-1</sup>) 2951, 1732, 1589, 1566, 1469, 1456, 1431, 1292, 1252, 742.



**2-(2-bromophenyl)propan-2-ol (14)** Methyl 2-bromobenzoate (5.00 mmol, 1.08 g, 1.00 eq.) were dissolved in 10 mL of anhydrous THF and cooled to 0 °C. Then methylmagnesium chloride (15.0 mmol, 5 mL, 3M in THF, 3.00 eq.) was added slowly *via* syringe over a period of 20 minutes. The solution was allowed to warm up to room temperature and stirred overnight. The so-obtained, white suspension was neutralized with saturated ammonium chloride solution, extracted with ethyl acetate and dried over magnesium sulfate. The evaporation of the solvent afforded the title compound as colorless oil. 1.07 g yield: 100%.

<sup>1</sup>H NMR (500 MHz, CDCl<sub>3</sub>) δ 7.67 (dd, *J* = 7.9, 1.8 Hz, 1H), 7.58 (dd, *J* = 7.9, 1.4 Hz, 1H), 7.30 (ddd, *J* = 7.9, 7.3, 1.4 Hz, 1H), 7.10 (ddd, *J* = 7.9, 7.3, 1.7 Hz, 1H), 1.75 (s, 6H). <sup>13</sup>C NMR (125 MHz, CDCl<sub>3</sub>) δ 146.13, 135.20, 128.66, 127.67, 127.36, 120.60, 73.69, 29.66. IR (cm<sup>-1</sup>) 3400, 3000, 2979, 2929, 1587, 1560, 1466, 1425, 1363, 1267, 1171, 1095, 754.

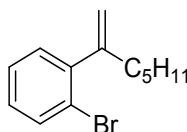


### 1-bromo-2-(prop-1-en-2-yl)benzene 1a

**Route A** Methyltriphenylphosphonium bromide (7.30 mmol, 2.61 g, 2.00 eq.) was suspended in tetrahydrofuran (30 mL) under argon and placed in ice/water bath. Then 2.5 M butyllithium solution (8.03 mmol, 3.2 mL, 2.20 eq.) was added dropwise until complete consumption of the phosphonium salt. The to the obtained yellow solution 1-(2-bromophenyl)ethanone (3.65 mmol, 0.73 g, 1.00 eq.) was added *via* syringe. The mixture was brought to room temperature and left stirring overnight. Then it was extracted with chloroform, dried over magnesium sulfate and chromatographed with hexane giving the title compound as colorless oil. 0.59 g yield: 82%.

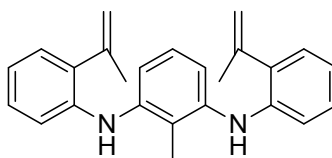
**Route B** 2-(2-bromophenyl)propan-2-ol (21.00 mmol, 4.54 g) were dissolved in a mixture of glacial acetic acid (6.4 mL) and acetic anhydride (0.5 mL). To the solution 1.6 mL of concentrated sulfuric acid were added and the solution was stirred over night in room temperature. Then it was neutralized with saturated sodium carbonate solution, extracted with ethyl acetate and dried over magnesium sulfate. Upon evaporation of the solvent 1-bromo-2-(prop-1-en-2-yl)benzene was obtained as colorless oil. 3.54 g yield: 86%.

**<sup>1</sup>H NMR** (500 MHz, CDCl<sub>3</sub>) δ 7.55 (dd, *J* = 8.0, 1.3 Hz, 1H), 7.26 (td, *J* = 7.4, 1.3 Hz, 1H), 7.19 (dd, *J* = 7.6, 1.8 Hz, 1H), 7.11 (ddd, *J* = 8.0, 7.4, 1.8 Hz, 1H), 5.23 (dq, *J* = 1.9, 1.6 Hz, 1H), 4.94 (dq, *J* = 1.9, 0.9 Hz, 1H), 2.10 (dd, *J* = 1.6, 0.9 Hz, 3H). **<sup>13</sup>C NMR** (100 MHz, CDCl<sub>3</sub>) δ 145.91, 144.96, 132.87, 129.83, 128.47, 127.34, 121.67, 116.13, 23.71. **IR** (KBr, cm<sup>-1</sup>) 3082, 2968, 2902, 1641, 1589, 1558, 1468, 1442, 1431, 1371, 901, 756.



**1-bromo-2-(hept-1-en-2-yl)benzene (1b)** Methyltriphenylphosphonium bromide (30.0 mmol, 10.73 g, 2.00 eq.) was suspended in tetrahydrofuran (60 mL) under argon and placed in ice/water bath. Then 2.5 M butyllithium solution (33.0 mmol, 13.2 mL, 2.20 eq.) was added dropwise until complete consumption of the phosphonium salt. The to the obtained yellow solution 1-(2-bromophenyl)hexan-1-one (15.0 mmol, 3.80 g, 1.00 eq.) was added dropwise *via* syringe. The mixture was brought to room temperature and left stirring overnight. Then it was extracted with chloroform, dried over magnesium sulfate and chromatographed with hexane to afford the title compound as colorless oil. 2.83 g yield: 75 %.

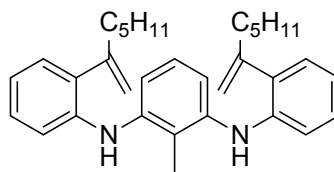
**<sup>1</sup>H NMR** (400 MHz, CDCl<sub>3</sub>) δ 7.55 (dd, *J* = 7.9, 1.2 Hz, 1H), 7.26 (td, *J* = 7.4, 1.2 Hz, 1H), 7.17 – 7.08 (m, 2H), 5.21 (q, *J* = 1.5 Hz, 1H), 4.97 – 4.92 (m, 1H), 2.44 – 2.38 (m, 2H), 1.47 – 1.33 (m, 2H), 1.34 – 1.13 (m, 4H), 0.87 (t, *J* = 7.1 Hz, 3H). **<sup>13</sup>C NMR** (100 MHz, CDCl<sub>3</sub>) δ 150.35, 144.28, 132.79, 130.39, 128.37, 127.10, 122.03, 114.90, 36.94, 31.65, 27.56, 22.69, 14.25. **IR** (cm<sup>-1</sup>) 3078, 3055, 2955, 2927, 2858, 1638, 1589, 1560, 1467, 1432, 903, 758. **Anal.** **Calcd.** for C<sub>13</sub>H<sub>17</sub>Br: C, 61.67; H, 6.77; Br, 31.56. Found: C, 60.52; H, 6.99.



**2-methyl-*N*<sup>1</sup>,*N*<sup>3</sup>-bis(2-(prop-1-en-2-yl)phenyl)benzene-1,3-diamine (2a)** In an oven-dried flask tris(dibenzylideneacetone)dipalladium(0) (0.76 mmol, 0.69 g, 2x3% mol) and tri-*tert*-butylphosphine (2.27 mmol, 0.46 g, 0.18 eq.) were dissolved in ca. 5 ml of anhydrous 1,4-dioxane under argon and allowed to stir for 15 minutes. To the solution of precatalyst 1-bromo-

2-(prop-1-en-2-yl)benzene (31.50 mmol, 6.22 g, 2.50 eq.), 2,6-diaminotoluene (12.60 mmol, 1.54 g, 1.00 eq.) and sodium *tert*-butanolate (37.80 mmol, 3.63 g, 3.00 eq.) in 25 mL of 1,4-dioxane were added under argon. The solution was heated to 110 °C overnight and the conversion was monitored on TLC. Upon cooling the suspension was extracted with ethyl acetate and dried over magnesium sulfate. Upon evaporation it was chromatographed with ethyl acetate (1%) and hexane to afford the title compound as yellow, viscous oil. 4.48 g yield: 100%.

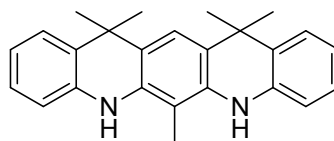
**<sup>1</sup>H NMR** (500 MHz, DMSO-*d*<sub>6</sub>) δ 7.12 – 7.09 (m, 4H), 6.96 (t, *J* = 8.0 Hz, 1H), 6.83 (td, *J* = 7.5, 1.2 Hz, 2H), 6.71 (dd, *J* = 8.6, 1.2 Hz, 2H), 6.61 (d, *J* = 8.0 Hz, 2H), 6.54 (s, 2H), 5.19 (dq, *J* = 2.9, 1.4 Hz, 1H), 5.05 (qd, *J* = 2.9, 0.9 Hz, 1H), 2.03 (dd, *J* = 1.4, 0.9 Hz, 6H), 1.97 (s, 3H). **<sup>13</sup>C NMR** (125 MHz, DMSO-*d*<sub>6</sub>) δ 143.74, 142.78, 141.46, 132.90, 128.66, 127.73, 126.12, 121.77, 119.84, 117.54, 115.63, 115.04, 23.01, 12.53. **IR** (KBr, cm<sup>-1</sup>) 3416, 3074, 3031, 2967, 2913, 2852, 2361, 2338, 1923, 1819, 1636, 1583, 1577, 1500, 1474, 1448, 1371, 1296, 1241, 1220, 1159, 1134, 1093, 1070, 1045, 1006, 905, 750, 709, 669, 565, 544, 483. **Anal. Calcd. for** C<sub>25</sub>H<sub>26</sub>N<sub>2</sub>: C, 84.70; H, 7.39; N, 7.90. Found: C, 84.86; H, 7.38; N, 7.91.



***N*<sup>1</sup>,*N*<sup>3</sup>-bis(2-(hept-1-en-2-yl)phenyl)-2-methylbenzene-1,3-diamine (2b)** The same procedure as for 2-methyl-*N*<sup>1</sup>,*N*<sup>3</sup>-bis(2-(prop-1-en-2-yl)phenyl)benzene-1,3-diamine incorporating palladium acetate (0.33 mmol, 73 mg 2x3% mol) tri-*tert*-butylphosphine (0.99 mmol, 0.20 g, 0.18 eq.) sodium *tert*-butanolate (16.35 mmol, 1.57 g, 3.00 eq.) 2,6-diaminotoluene (5.45 mmol, 0.67 g, 1.00 eq.) and 1-bromo-2-(hept-1-en-2-yl)benzene (12.0 mmol, 3.03 g, 2.20 eq.) in anhydrous toluene (20 mL) afforded after purification the title compound as yellow oil. 2.54 g, yield: 82 %.

**<sup>1</sup>H NMR** (400 MHz, DMSO-*d*<sub>6</sub>) δ 7.13 – 7.03 (m, 4H), 6.96 (t, *J* = 7.9 Hz, 1H), 6.82 (td, *J* = 7.4, 1.2 Hz, 2H), 6.73 – 6.70 (m, 2H), 6.63 (d, *J* = 7.9 Hz, 2H), 6.45 (s, 2H), 5.24 – 5.16 (m, 2H), 5.06 – 4.99 (m, 2H), 2.37 (t, *J* = 7.4 Hz, 4H), 1.95 (s, *J* = 14.1 Hz, 3H), 1.37 – 1.12 (m, 12H), 0.78 (t, *J* = 7.1 Hz, 6H). **<sup>13</sup>C NMR** (100 MHz, DMSO-*d*<sub>6</sub>) δ 148.38, 142.56, 141.44, 131.98, 129.14, 127.61, 126.14, 121.52, 119.65, 117.11, 114.92, 114.79, 35.94, 30.98, 27.21, 21.96, 13.90, 12.36. **IR** (cm<sup>-1</sup>) 3418, 3072, 3025, 2954, 2926, 2856, 1632, 1575, 1473, 1449, 1498,

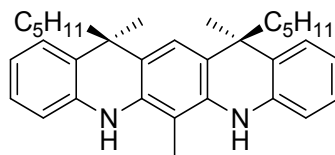
1299, 905, 745. **Anal. Calcd. for** C<sub>33</sub>H<sub>42</sub>N<sub>2</sub>: C, 84.93; H, 9.07; N, 6.00. Found: C, 85.00; H, 9.02; N, 5.19.



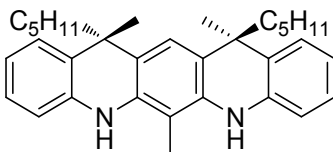
**6,12,12,14,14-pentamethyl-5,7,12,14-tetrahydroquinolino[3,2-*b*]acridine (3a)** 2-methyl-*N*<sup>1</sup>,*N*<sup>3</sup>-bis(2-(prop-1-en-2-yl)phenyl)benzene-1,3-diamine (12.60 mmol, 4.48 g) was diluted with glacial acetic acid (125 mL) and purged with argon for 20 minutes. Then to the mixture phosphoric acid (40 mL, 85% w/w) was added and the solution was purged with argon for another 20 minutes. Then it was allowed to stir at 100 °C in an oil bath for 0.5 h and after that period the heating was immediately ceased. The suspension was diluted with water and neutralized with saturated sodium carbonate solution. Then it was extracted with dichloromethane and dried over magnesium sulfate. Upon evaporation of the solvents the crude solid was chromatographed using hexane/dichloromethane (2/1) mixture to obtain the title compound as yellow solid. 2.96 g yield: 66%

<sup>1</sup>H NMR (500 MHz, DMSO-*d*<sub>6</sub>) δ 7.78 (s, 2H), 7.32 (dd, *J* = 7.8, 1.3 Hz, 2H), 7.21 (s, 1H), 7.10 (dd, *J* = 8.0, 1.3 Hz, 2H), 7.02 (ddd, *J* = 8.0, 7.2, 1.3 Hz, 2H), 6.78 (ddd, *J* = 7.8, 7.2, 1.3 Hz, 2H), 2.24 (s, 3H), 1.48 (s, 12H). <sup>13</sup>C NMR (125 MHz, DMSO-*d*<sub>6</sub>) δ 139.10, 134.93, 128.59, 126.13, 125.02, 120.21, 119.42, 119.40, 114.34, 102.74, 35.45, 31.43, 10.85. IR (KBr, cm<sup>-1</sup>) 3450, 3421, 3058, 3027, 2957, 2921, 2855, 2562, 1893, 1772, 1674, 1606, 1586, 1492, 1464, 1448, 1384, 1362, 1357, 1323, 1302, 1280, 1266, 1247, 1224, 1198, 1157, 1135, 1120, 1110, 1098, 1187, 1039, 1001, 974, 965, 937, 930, 914, 881, 846, 815, 744, 678, 606, 584, 560, 547, 525, 498, 483, 465, 449, 407. **Anal. Calcd. for** C<sub>25</sub>H<sub>26</sub>N<sub>2</sub>: C, 84.70; H, 7.39; N, 7.90. Found: C, 83.90; H, 7.32; N, 7.60.

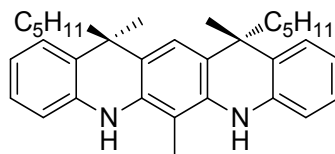
**(12*R*,14*S*)-6,12,14-trimethyl-12,14-dipentyl-5,7,12,14-tetrahydroquinolino[3,2-*b*]acridine**



**(12*S*,14*S*)-6,12,14-trimethyl-12,14-dipentyl-5,7,12,14-tetrahydroquinolino[3,2-*b*]acridine**



**(12*R*,14*R*)-6,12,14-trimethyl-12,14-dipentyl-5,7,12,14-tetrahydroquinolino[3,2-*b*]acridine**



**6,12,14-trimethyl-12,14-dipentyl-5,7,12,14-tetrahydroquinolino[3,2-*b*]acridine (3b)** The same procedure as for 6,12,12,14,14-pentamethyl-5,7,12,14-tetrahydroquinolino[3,2-*b*]acridine involving *N*<sup>1</sup>,*N*<sup>3</sup>-bis(2-(hept-1-en-2-yl)phenyl)-2-methylbenzene-1,3-diamine (1.00 mmol, 0.47 g), glacial acetic acid (3 mL) and phosphoric acid (4.5 mL, 85% w/w) after 4 hours of heating at 100 °C afforded a violet slurry, which was neutralized with 1M sodium hydroxide solution. Then after extraction with diethyl ether and drying over sodium sulfate the crude mixture was chromatographed with hexane/dichloromethane (2/1), where the 2 diastereomers were resolved afterwards to afford (12*R*,14*S*)-6,12,14-trimethyl-12,14-dipentyl-5,7,12,14-tetrahydroquinolino[3,2-*b*]acridine (*meso* form) as white solid (*R*<sub>f</sub> = 0.15) and a mixture of enantiomers: (12*R*,14*R*)- and (12*S*,14*S*)-6,12,14-trimethyl-12,14-dipentyl-5,7,12,14-tetrahydroquinolino[3,2-*b*]acridine as yellow solidified oil (*R*<sub>f</sub> = 0.18). overall mass of two diastereomers: 0.20 g, yield: 43%.

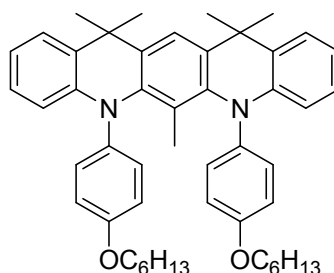
**(12*R*,14*S*)-6,12,14-trimethyl-12,14-dipentyl-5,7,12,14-tetrahydroquinolino[3,2-*b*]acridine**

<sup>1</sup>H NMR (400 MHz, acetone-*d*<sub>6</sub>) δ 7.31 (dd, *J* = 7.8, 1.3 Hz, 2H), 7.20 (s, 1H), 7.18 (s, 2H), 7.00 (ddd, *J* = 8.0, 7.0, 1.3 Hz, 2H), 6.94 (dd, *J* = 8.0, 1.5 Hz, 2H), 6.79 (ddd, *J* = 7.8, 7.0, 1.5 Hz, 2H), 2.19 (s, 3H), 1.96 – 1.86 (m, 4H), 1.60 (s, 6H), 1.22 – 0.94 (m, 12H), 0.76 (t, *J* = 7.0

Hz, 6H).  $^{13}\text{C}$  NMR (100 MHz, acetone- $d_6$ )  $\delta$  140.35, 136.15, 127.92, 127.03, 126.75, 122.48, 120.34, 119.17, 114.83, 102.53, 45.96, 40.43, 33.23, 32.82, 26.05, 23.40, 14.43, 10.35.

**(12*S*,14*S*)-6,12,14-trimethyl-12,14-dipentyl-5,7,12,14-tetrahydroquinolino[3,2-*b*]acridine**  
+ **(12*R*,14*R*)-6,12,14-trimethyl-12,14-dipentyl-5,7,12,14-tetrahydroquinolino[3,2-*b*]acridine**

$^1\text{H}$  NMR (400 MHz, acetone- $d_6$ )  $\delta$  7.32 (dd,  $J = 7.8, 1.4$  Hz, 2H), 7.21 (s, 1H), 7.19 (s, 2H), 7.01 (ddd,  $J = 8.0, 7.0, 1.4$  Hz, 2H), 6.94 (dd,  $J = 8.0, 1.5$  Hz, 2H), 6.80 (ddd,  $J = 7.8, 7.0, 1.5$  Hz, 2H), 2.21 (s, 3H), 1.98 – 1.84 (m, 4H), 1.60 (s, 6H), 1.23 – 0.95 (m, 12H), 0.74 (t,  $J = 7.0$  Hz, 6H).  $^{13}\text{C}$  NMR (100 MHz, acetone- $d_6$ )  $\delta$  140.45, 136.20, 127.89, 127.02, 126.73, 122.28, 120.34, 119.39, 114.85, 102.62, 45.39, 40.46, 32.92, 32.41, 25.63, 23.11, 14.29, 10.34. IR (cm $^{-1}$ ) 3448, 3039, 2952, 2926, 2856, 1606, 1587, 1465, 1489, 1318, 744. **Anal. Calcd. for** C<sub>33</sub>H<sub>42</sub>N<sub>2</sub>: C, 84.93; H, 9.07; N, 6.00. Found: C, 84.83; H, 9.06; N, 6.04. **MS** (EI+, m/z) [M $^+$ ] 466.

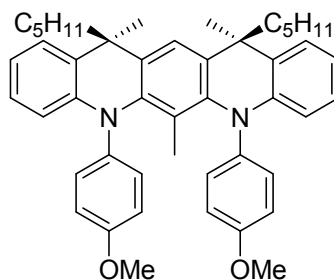


**5,7-bis(4-(hexyloxy)phenyl)-6,12,12,14,14-pentamethyl-5,7,12,14-tetrahydroquinolino[3,2-*b*]acridine (4a)** In an oven-dried flask palladium acetate (0.09 mmol, 20 mg, 2x3% mol) and tri-*tert*-butylphosphine (0.27 mmol, 55 mg, 0.18 eq.) were mixed under argon, diluted with ca. 3 mL of anhydrous toluene and left stirring. Then the flask was charged with 1-(hexyloxy)-4-iodobenzene (3.75 mmol, 1.14 g, 2.50 eq.), 6,12,12,14,14-pentamethyl-5,7,12,14-tetrahydroquinolino[3,2-*b*]acridine (1.50 mmol, 0.53 g, 1.00 eq.) and sodium *tert*-butanolate (4.50 mmol, 0.43 g, 3.00 eq.). The mixture was diluted with another 7 mL of toluene and heated to 110 °C with continuous stirring overnight. Then the reaction was quenched with water and extracted with ethyl acetate. Upon drying over magnesium sulfate the crude solid was chromatographed with hexane/dichloromethane (2/1) mixture to afford the title product as white solid. 0.89 g yield: 84%.

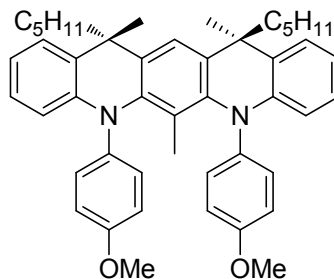
$^1\text{H}$  NMR (500 MHz, acetone- $d_6$ )  $\delta$  7.63 (dd,  $J = 8.0, 1.2$  Hz, 2H), 7.60 (s, 1H), 7.50 (dd,  $J = 7.8, 1.5$  Hz, 2H), 7.29 – 7.20 (m, 2H), 7.13 (ddd,  $J = 7.8, 7.6, 1.2$  Hz, 2H), 7.08 (d,  $J = 9.1$  Hz, 4H), 6.87 (d,  $J = 9.2$  Hz, 4H), 3.92 (t,  $J = 6.5$  Hz, 4H), 1.90 (s,  $J = 5.1$  Hz, 3H), 1.80 – 1.66 (m,

4H), 1.59 (s, 12H), 1.50 – 1.40 (m, 4H), 1.40 – 1.27 (m, 8H), 0.90 (t,  $J = 7.1$  Hz, 6H).  $^{13}\text{C}$  NMR (125 MHz, acetone- $d_6$ )  $\delta$  154.85, 144.39, 143.41, 141.51, 141.44, 139.59, 128.25, 126.77, 125.63, 125.10, 125.04, 119.73, 118.55, 115.65, 68.79, 38.57, 32.37, 30.13, 29.38, 26.52, 23.29, 16.12, 14.32. **IR** (KBr,  $\text{cm}^{-1}$ ) 3421, 3048, 3030, 2952, 2926, 2859, 1587, 1507, 1479, 1471, 1453, 1428, 1386, 1377, 1364, 1311, 1287, 1266, 1243, 1190, 1179, 1167, 1145, 1128, 1118, 1097, 1184, 1074, 1040, 1020, 999, 979, 938, 905, 871, 851, 819, 792, 779, 753, 745, 705, 675, 642, 626, 615, 588, 551, 517. **Anal. Calcd.** for  $\text{C}_{49}\text{H}_{58}\text{N}_2\text{O}_2$ : C, 83.24; H, 8.27; N, 3.96; O, 4.53. Found: C, 83.27; H, 8.20; N, 3.96. **HRMS** (TOF MS ES+) Anal. Calcd. for  $\text{C}_{49}\text{H}_{58}\text{N}_2\text{O}_2\text{Na}$ : 729.4396 Found: 729.4387  $[\text{M}+\text{Na}]^+$

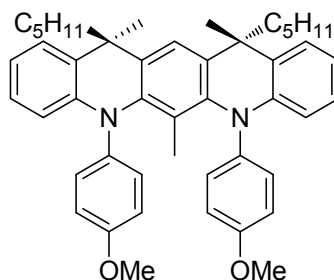
**(12*R*,14*S*)-5,7-bis(4-methoxyphenyl)-6,12,14-trimethyl-12,14-dipentyl-5,7,12,14-tetrahydroquinolino[3,2-*b*]acridine**



**(12*S*,14*S*)-5,7-bis(4-methoxyphenyl)-6,12,14-trimethyl-12,14-dipentyl-5,7,12,14-tetrahydroquinolino[3,2-*b*]acridine**



**(12*R*,14*R*)-5,7-bis(4-methoxyphenyl)-6,12,14-trimethyl-12,14-dipentyl-5,7,12,14-tetrahydroquinolino[3,2-*b*]acridine**



**5,7-bis(4-methoxyphenyl)-6,12,14-trimethyl-12,14-dipentyl-5,7,12,14-tetrahydroquinolino[3,2-*b*]acridine (4b)** The reaction was repeated on each of the separated diastereomers. The same procedure as applied in the case of 5,7-bis(4-(hexyloxy)phenyl)-6,12,14,14-pentamethyl-5,7,12,14-tetrahydroquinolino[3,2-*b*]acridine incorporating palladium acetate (0.08 mmol, 18 mg, 2x5% mol) tri-*tert*-butylphosphine (0.25 mmol, 50 mg, 0.30 eq.) sodium *tert*-butanolate (2.45 mmol, 0.24 g, 3.00 eq.), 12,14-trimethyl-12,14-dipentyl-5,7,12,14-tetrahydroquinolino[3,2-*b*]acridine (0.82 mmol, 0.38 g, 1.00 eq.) and 4-iodoanisole (1.80 mmol, 0.42 g, 2.20 eq.) in anhydrous toluene (15 mL) afforded upon purification *via* chromatography the title compound as white solid. 0.51 g yield: 95%.

**(12*R*,14*S*)-5,7-bis(4-methoxyphenyl)-6,12,14-trimethyl-12,14-dipentyl-5,7,12,14-tetrahydroquinolino[3,2-*b*]acridine**

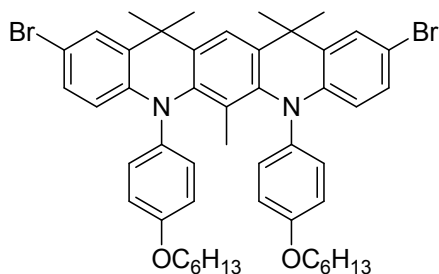
<sup>1</sup>H NMR (400 MHz, acetone-*d*<sub>6</sub>) δ 7.59 (dd, *J* = 7.9, 1.0 Hz, 2H), 7.51 – 7.43 (m, 3H), 7.22 (ddd, *J* = 7.9, 7.3, 1.3 Hz, 2H), 7.18 – 7.04 (m, 6H), 6.86 (d, *J* = 9.1 Hz, 4H), 3.73 (s, 6H), 1.84 (s, 3H), 1.80 (s, 6H), 1.74 – 1.57 (m, 4H), 1.36 – 0.94 (m, 12H), 0.73 (t, *J* = 7.0 Hz, 6H). <sup>13</sup>C NMR (100 MHz, acetone-*d*<sub>6</sub>) δ 155.46, 144.20, 141.79, 141.66, 141.50, 136.55, 126.99, 126.57, 125.85, 124.87, 124.53, 121.09, 120.79, 114.76, 55.68, 44.21, 41.93, 32.73, 25.52, 24.33, 22.93, 16.65, 14.30.

**(12*R*,14*R*)-5,7-bis(4-methoxyphenyl)-6,12,14-trimethyl-12,14-dipentyl-5,7,12,14-tetrahydroquinolino[3,2-*b*]acridine** +

**(12*S*,14*S*)-5,7-bis(4-methoxyphenyl)-6,12,14-trimethyl-12,14-dipentyl-5,7,12,14-tetrahydroquinolino[3,2-*b*]acridine**

<sup>1</sup>H NMR (400 MHz, acetone-*d*<sub>6</sub>) δ 7.57 (dd, *J* = 8.0, 1.2 Hz, 2H), 7.49 (s, 1H), 7.48 (dd, *J* = 7.9, 1.4 Hz, 2H), 7.22 (ddd, *J* = 8.0, 7.3, 1.4 Hz, 2H), 7.11 (ddd, *J* = 7.9, 7.3, 1.2 Hz, 2H), 7.04 (d, *J* = 9.2 Hz, 4H), 6.82 (d, *J* = 9.2 Hz, 4H), 3.73 (s, *J* = 11.3 Hz, 6H), 1.92 – 1.80 (m, 4H), 1.78 (d, *J* = 4.6 Hz, 3H), 1.72 (s, 6H), 1.15 – 0.97 (m, 12H), 0.71 (t, *J* = 6.0 Hz, 6H). <sup>13</sup>C NMR (100 MHz, acetone-*d*<sub>6</sub>) δ 155.73, 144.59, 142.13, 141.83, 140.37, 136.16, 126.67, 126.34, 126.19,

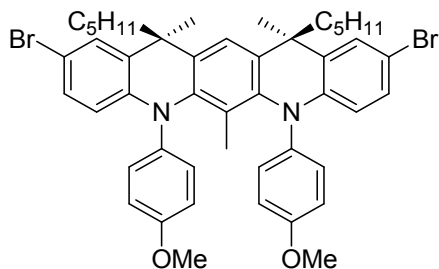
124.64, 124.45, 122.06, 120.76, 114.69, 55.66, 42.06, 41.88, 32.76, 28.51, 25.33, 22.86, 16.90, 14.27. **IR** (cm<sup>-1</sup>) 3048, 2951, 2931, 2856, 1583, 1504, 1452, 1284, 1240, 1037, 822, 753. **Anal.** **Calcd.** for C<sub>47</sub>H<sub>54</sub>N<sub>2</sub>O<sub>2</sub>: C, 83.14; H, 8.02; N, 4.13; O, 4.71. Found: C, 83.12; H, 8.06; N, 4.15. **MS** (EI+, m/z) [M<sup>+</sup>] 678 .



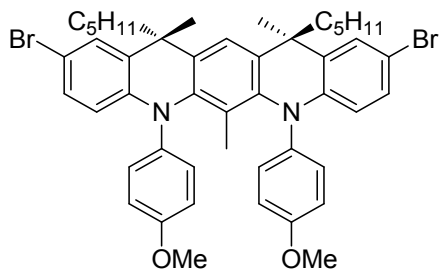
**2,10-dibromo-5,7-bis(4-(hexyloxy)phenyl)-6,12,12,14,14-pentamethyl-5,7,12,14-tetrahydroquinolino[3,2-*b*]acridine (5a)** An oven-dried flask was charged with 5,7-bis(4-(hexyloxy)phenyl)-6,12,12,14,14-pentamethyl-5,7,12,14-tetrahydroquinolino[3,2-*b*]acridine (1.16 mmol, 0.82 g, 1.00 eq.) and diluted with anhydrous DMF (10 mL) under argon. The mixture was cooled to 0 °C and then *N*-bromosuccinimide (2.54 mmol, 0.45 g, 2.20 eq.) in DMF (10 mL) was added dropwise over a period of 20 minutes. Upon completion of the addition the ice-bath was removed and the solution was allowed to stir overnight. When finished, the reaction was quenched with water and extracted with ethyl acetate. The organic layer was dried over magnesium sulfate and the crude slurry was chromatographed with hexane/dichloromethane (3/1) mixture to afford the title compound as white solid. 0.94 g. yield: 94%

**<sup>1</sup>H NMR** (500 MHz, acetone-*d*<sub>6</sub>) δ 7.63 (d, *J* = 2.3 Hz, 2H), 7.60 (s, 1H), 7.58 (d, *J* = 8.6 Hz, 2H), 7.40 (dd, *J* = 8.5, 2.3 Hz, 2H), 7.08 (d, *J* = 9.3 Hz, 4H), 6.87 (d, *J* = 9.3 Hz, 4H), 3.93 (t, *J* = 6.5 Hz, 4H), 1.79 (s, 3H), 1.77 – 1.68 (m, 4H), 1.61 (s, 12H), 1.56 – 1.38 (m, 4H), 1.39 – 1.29 (m, 8H), 0.94 – 0.84 (m, 6H). **<sup>13</sup>C NMR** (125 MHz, acetone-*d*<sub>6</sub>) δ 155.37, 145.24, 143.69, 141.40, 141.00, 138.42, 129.79, 128.22, 127.51, 126.78, 121.01, 118.84, 117.41, 115.68, 68.79, 38.67, 32.36, 30.09, 29.47, 26.51, 23.29, 16.53, 14.33. **IR** (KBr, cm<sup>-1</sup>) 2956, 2929, 2860, 1580, 1507, 1476, 1467, 1459, 1428, 1418, 1398, 1363, 1310, 1291, 1241, 1209, 1188, 1164, 1128, 1085, 1030, 978, 937, 906, 890, 875, 863, 815, 792, 725, 691, 674, 635, 605, 595, 522. **Anal.** **Calcd.** for C<sub>49</sub>H<sub>56</sub>Br<sub>2</sub>N<sub>2</sub>O<sub>2</sub>: C, 68.05; H, 6.53; Br, 18.48; N, 3.24; O, 3.70. Found: C, 68.06; H, 6.52; N, 3.27. **HRMS** (TOF MS ES+) Anal. Calcd. for C<sub>49</sub>H<sub>56</sub>Br<sub>2</sub>N<sub>2</sub>O<sub>2</sub>: 862.2709 Found: 862.2722 [M]<sup>+</sup>

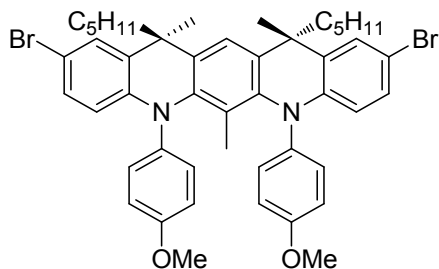
**(12*R*,14*S*)-2,10-dibromo-5,7-bis(4-methoxyphenyl)-6,12,14-trimethyl-12,14-dipentyl-5,7,12,14-tetrahydroquinolino[3,2-*b*]acridine**



**(12*S*,14*S*)-2,10-dibromo-5,7-bis(4-methoxyphenyl)-6,12,14-trimethyl-12,14-dipentyl-5,7,12,14-tetrahydroquinolino[3,2-*b*]acridine**



**(12*R*,14*R*)-2,10-dibromo-5,7-bis(4-methoxyphenyl)-6,12,14-trimethyl-12,14-dipentyl-5,7,12,14-tetrahydroquinolino[3,2-*b*]acridine**



**2,10-dibromo-5,7-bis(4-methoxyphenyl)-6,12,14-trimethyl-12,14-dipentyl-5,7,12,14-tetrahydroquinolino[3,2-*b*]acridine (5b)** The same procedure as for bromination of 5,7-bis(4-(hexyloxy)phenyl)-6,12,12,14,14-pentamethyl-5,7,12,14-tetrahydroquinolino[3,2-*b*]acridine was repeated using: 5,7-bis(4-methoxyphenyl)-6,12,14-trimethyl-12,14-dipentyl-5,7,12,14-tetrahydroquinolino[3,2-*b*]acridine (0.60 mmol, 0.41 g, 1.00 eq.) and *N*-bromosuccinimide (1.32 mmol, 0.24 g, 2.20 eq.) in

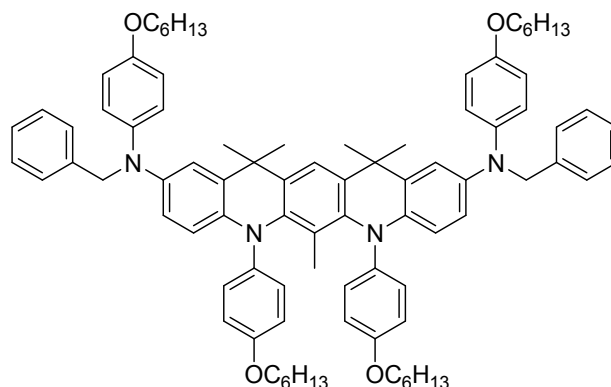
anhydrous DMF (15 mL) afforded upon chromatography (hexane/dichloromethane 2/1) the title product as white solid. 0.49 g, yield: 98%.

**(12*R*,14*S*)-2,10-dibromo-5,7-bis(4-methoxyphenyl)-6,12,14-trimethyl-12,14-dipentyl-5,7,12,14-tetrahydroquinolino[3,2-*b*]acridine**

<sup>1</sup>H NMR (400 MHz, acetone-*d*<sub>6</sub>) δ 7.59 (d, *J* = 2.3 Hz, 2H), 7.52 (d, *J* = 8.6 Hz, 2H), 7.44 (s, 1H), 7.36 (dd, *J* = 8.6, 2.3 Hz, 2H), 7.07 (d, *J* = 9.2 Hz, 4H), 6.86 (d, *J* = 9.2 Hz, 4H), 3.74 (s, 6H), 1.81 (s, 6H), 1.73 – 1.55 (m, 7H), 1.32 – 1.16 (m, 4H), 1.16 – 0.93 (m, 8H), 0.73 (t, *J* = 7.0 Hz, 6H). <sup>13</sup>C NMR (100 MHz, acetone-*d*<sub>6</sub>) δ 156.03, 143.55, 143.47, 141.50, 141.27, 135.17, 129.63, 128.86, 126.10, 125.94, 122.24, 121.39, 116.91, 114.86, 55.71, 44.41, 42.06, 32.66, 25.51, 24.82, 22.94, 17.15, 14.26.

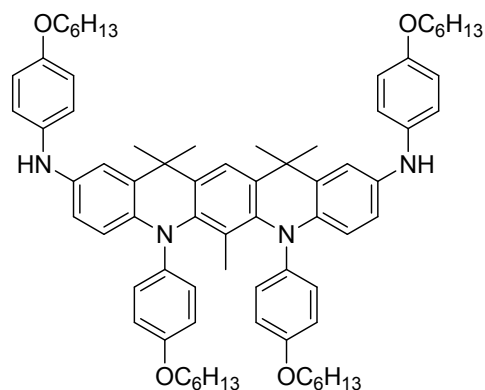
**(12*R*,14*R*)-2,10-dibromo-5,7-bis(4-methoxyphenyl)-6,12,14-trimethyl-12,14-dipentyl-5,7,12,14-tetrahydroquinolino[3,2-*b*]acridine** +  
**(12*S*,14*S*)-2,10-dibromo-5,7-bis(4-methoxyphenyl)-6,12,14-trimethyl-12,14-dipentyl-5,7,12,14-tetrahydroquinolino[3,2-*b*]acridine**

<sup>1</sup>H NMR (400 MHz, acetone-*d*<sub>6</sub>) δ 7.60 (d, *J* = 2.3 Hz, 2H), 7.50 (d, *J* = 8.6 Hz, 2H), 7.48 (s, 1H), 7.35 (dd, *J* = 8.6, 2.3 Hz, 2H), 7.04 (d, *J* = 9.2 Hz, 4H), 6.83 (d, *J* = 9.2 Hz, 4H), 3.73 (s, 6H), 1.94 – 1.81 (m, 4H), 1.74 (s, 6H), 1.67 (s, 3H), 1.17 – 1.02 (m, 12H), 0.72 (t, *J* = 6.3 Hz, 6H). <sup>13</sup>C NMR (100 MHz, acetone-*d*<sub>6</sub>) δ 156.24, 143.90, 142.16, 141.76, 141.69, 134.87, 129.71, 129.10, 125.79, 125.57, 123.33, 120.94, 116.80, 114.80, 55.69, 42.15, 42.02, 32.65, 28.90, 25.29, 22.82, 17.41, 14.25. IR (cm<sup>-1</sup>) 3054, 2952, 2920, 2859, 1606, 1505, 1461, 1279, 1240, 1037, 819. **Anal. Calcd. for** C<sub>47</sub>H<sub>52</sub>Br<sub>2</sub>N<sub>2</sub>O<sub>2</sub>: C, 67.46; H, 6.26; Br, 19.10; N, 3.35; O, 3.82. Found: C, 67.62; H, 6.27; N, 3.33. **HRMS** (TOF MS ES<sup>+</sup>) Anal. Calcd. for C<sub>47</sub>H<sub>52</sub>Br<sub>2</sub>N<sub>2</sub>O<sub>2</sub>: 834.2385 Found: 834.2396 [M<sup>+</sup>]



***N*<sup>2</sup>,*N*<sup>10</sup>-dibenzyl-*N*<sup>2</sup>,*N*<sup>10</sup>,5,7-tetrakis(4-(hexyloxy)phenyl)-6,12,12,14,14-pentamethyl-5,7,12,14-tetrahydroquinolino[3,2-*b*]acridine-2,10-diamine (6)** An oven-dried flask was charged with palladium acetate (0.038 mmol, 8 mg, 2x3% mol), tri-*tert*-butylphosphine (0.11 mmol, 23 mg, 0.18 eq.) and diluted with ca. 3 mL of anhydrous toluene. The solution was allowed to stir for 10 minutes and then 2,10-dibromo-5,7-bis(4-(hexyloxy)phenyl)-6,12,12,14,14-pentamethyl-5,7,12,14-tetrahydroquinolino[3,2-*b*]acridine (0.63 mmol, 0.54 g, 1.00 eq.), *N*-benzyl-4-(hexyloxy)aniline (1.57 mmol, 0.45 g, 2.50 eq.) and sodium *tert*-butanolate (1.89 mmol, 0.18 g, 3.00 eq.) were added, respectively. The mixture was diluted with another 7 mL of toluene and heated to 110 °C overnight. Then the reaction was quenched with water and extracted with ethyl acetate. The organic layer was dried over magnesium sulfate and the resulting slurry was chromatographed using hexane/dichloromethane (2/1) mixture to afford the title compound as yellow solid. 0.62 g yield: 84%.

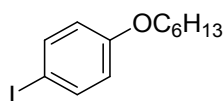
**<sup>1</sup>H NMR** (500 MHz, acetone-*d*<sub>6</sub>) δ 7.44 (s, 1H), 7.42 – 7.35 (m, 6H), 7.31 – 7.25 (m, 4H), 7.22 – 7.15 (m, 2H), 7.12 (d, *J* = 9.0 Hz, 4H), 7.01 (d, *J* = 2.7 Hz, 2H), 6.98 (d, *J* = 9.2 Hz, 4H), 6.88 (d, *J* = 9.0 Hz, 4H), 6.82 (d, *J* = 9.2 Hz, 4H), 6.74 (dd, *J* = 8.7, 2.7 Hz, 2H), 4.95 (s, 4H), 3.94 (t, *J* = 6.5 Hz, 4H), 3.89 (t, *J* = 6.5 Hz, 4H), 1.93 (s, 3H), 1.81 – 1.65 (m, 8H), 1.52 – 1.38 (m, 20H), 1.37 – 1.26 (m, 16H), 0.96 – 0.86 (m, 12H). **<sup>13</sup>C NMR** (125 MHz, acetone-*d*<sub>6</sub>) δ 156.23, 154.25, 146.65, 144.76, 142.33, 141.87, 141.78, 140.66, 140.11, 136.56, 129.24, 129.09, 127.64, 127.49, 126.86, 125.87, 118.40, 118.24, 116.15, 115.72, 115.64, 114.14, 68.77, 68.75, 57.52, 38.94, 32.37, 32.35, 30.15, 30.08, 28.96, 26.52, 26.49, 23.29, 15.55, 14.33. **IR** (KBr, cm<sup>-1</sup>) 3061, 3041, 2953, 2928, 2858, 1606, 1581, 1560, 1507, 1471, 1459, 1429, 1378, 1351, 1269, 1241, 1216, 1127, 1100, 1064, 1028, 1004, 936, 907, 888, 819, 724, 695, 645, 603, 581, 522, 456. **Anal.** **Calcd. for** C<sub>87</sub>H<sub>104</sub>N<sub>4</sub>O<sub>4</sub>: C, 82.29; H, 8.26; N, 4.41; O, 5.04. Found: C, 82.26; H, 8.31; N, 4.56. **HRMS** (TOF MS ES<sup>+</sup>) **Anal.** **Calcd. for** C<sub>87</sub>H<sub>105</sub>N<sub>4</sub>O<sub>4</sub>: 1269.8156 Found: 1269.8136 [M+H]<sup>+</sup>



***N*<sup>2</sup>,*N*<sup>10</sup>,5,7-tetrakis(4-(hexyloxy)phenyl)-6,12,12,14,14-pentamethyl-5,7,12,14-tetrahydroquinolino[3,2-*b*]acridine-2,10-diamine (7)**

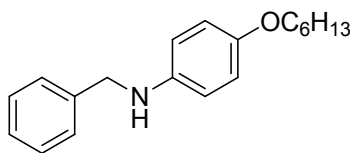
*N*<sup>2</sup>,*N*<sup>10</sup>-dibenzyl-*N*<sup>2</sup>,*N*<sup>10</sup>,5,7-tetrakis(4-(hexyloxy)phenyl)-6,12,12,14,14-pentamethyl-5,7,12,14-tetrahydroquinolino[3,2-*b*]acridine-2,10-diamine (0.50 mmol, 0.63 g, 1.00 eq.) was mixed with 10% Pd/C (0.20 g) and ammonium formate (7.50 mmol, 0.47 g, 15.0 eq.) in methanol (10 mL). The suspension was purged with argon for 20 minutes and then heated to 80 °C for 4 hours. Upon cooling the mixture was filtrated and after evaporation of the solvent it was chromatographed with hexane/dichloromethane (2/1) to afford the title compound as colorless solid. 0.49 g yield: 90%.

<sup>1</sup>H NMR (500 MHz, DMSO-*d*<sub>6</sub>) δ 7.80 (s, 2H), 7.43 (s, 1H), 7.39 (d, *J* = 8.5 Hz, 2H), 7.05 (d, *J* = 2.2 Hz, 2H), 7.00 (d, *J* = 9.0 Hz, 4H), 6.89 (d, *J* = 9.2 Hz, 4H), 6.86 (dd, *J* = 8.5, 2.2 Hz, 2H), 6.84 – 6.78 (m, 8H), 3.89 – 3.82 (m, 8H), 1.86 (s, 3H), 1.71 – 1.59 (m, 8H), 1.45 (s, *J* = 33.9 Hz, 12H), 1.42 – 1.32 (m, 8H), 1.32 – 1.20 (m, 16H), 0.93 – 0.80 (m, 12H). <sup>13</sup>C NMR (125 MHz, DMSO) δ 152.83, 152.54, 144.04, 141.65, 140.49, 140.40, 139.01, 136.65, 134.52, 127.83, 126.20, 119.37, 117.44, 116.58, 115.14, 114.79, 112.44, 111.34, 67.63, 67.56, 37.77, 31.04, 28.82, 28.80, 28.21, 25.25, 25.24, 22.08, 22.06, 14.67, 13.89, 13.86. IR (KBr, cm<sup>-1</sup>) 3393, 3040, 2953, 2930, 2858, 1608, 1566, 1508, 1471, 1427, 1390, 1361, 1282, 1240, 1191, 1147, 1127, 1104, 1074, 1031, 938, 905, 820, 726, 675, 645, 604, 582, 519. Anal. Calcd. for C<sub>73</sub>H<sub>92</sub>N<sub>4</sub>O<sub>4</sub>: C, 80.47; H, 8.51; N, 5.14; O, 5.87. Found: C, 80.21; H, 8.44; N, 5.15. HRMS (TOF MS ES+) Anal. Calcd. for C<sub>73</sub>H<sub>93</sub>N<sub>4</sub>O<sub>4</sub>: 1089.7197 Found: 1089.7219 [M+H]<sup>+</sup>



**1-(hexyloxy)-4-iodobenzene (15)** 4-iodophenol (5.00 mmol, 1.10 g, 1.00 eq.), 1-bromohexane (4.75 mmol, 0.78 g, 0.95 eq.) and potassium carbonate (10.0 mmol, 1.38 g, 2.00 eq.) were refluxed in acetone (10 mL) overnight. Then the reaction was quenched with addition of water and extracted with ethyl acetate. Upon drying over magnesium sulfate and evaporation the crude product was chromatographed with hexane to obtain the title compound as colorless oil. 1.14 g yield: 79%

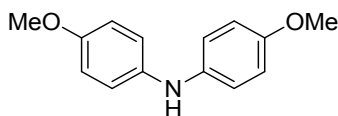
$^1\text{H NMR}$  (400 MHz,  $\text{CDCl}_3$ )  $\delta$  7.54 (d,  $J = 9.0$  Hz, 2H), 6.67 (d,  $J = 9.0$  Hz, 2H), 3.91 (t,  $J = 6.6$  Hz, 2H), 1.82 – 1.69 (m, 2H), 1.52 – 1.39 (m, 2H), 1.39 – 1.24 (m, 4H), 0.91 (t,  $J = 7.1$  Hz, 3H).  $^{13}\text{C NMR}$  (125 MHz,  $\text{CDCl}_3$ )  $\delta$  159.16, 138.28, 117.08, 82.52, 68.28, 31.70, 29.26, 25.82, 22.73, 14.17. **IR** ( $\text{cm}^{-1}$ ) 2954, 2929, 2870, 2856, 1585, 1571, 1485, 1465, 1430, 1391, 1380, 1302, 1280, 1241, 1174, 1116, 1099, 1063, 1027, 997, 816, 800, 728, 694, 630, 589, 503.



**N-benzyl-4-(hexyloxy)aniline (8)** 4-(hexyloxy)aniline (5.00 mmol, 0.97 g, 1.00 eq.) was dissolved in methanol (150 mL) and the solution was purged with argon for 20 minutes. Then benzaldehyde (12.0 mmol, 1.27 g, 2.40 eq.) was introduced and the whole was allowed to stir for 30 minutes. Then sodium cyanoborohydride (17.50 mmol, 1.10 g, 3.50 eq.) was added in one portion, which was followed by the addition of 5 drops of acetic acid. The reaction mixture was then stirred for another hour at room temperature and then the solvent was evaporated to reduce its volume to about 1/3. The crude product was then extracted with ethyl acetate and dried over magnesium sulfate. Then upon evaporation of the solvent it was chromatographed with hexane to afford the title compound as white solid. 1.21 g yield: 85%

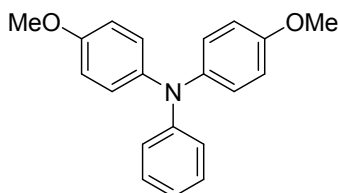
$^1\text{H NMR}$  (500 MHz,  $\text{DMSO-}d_6$ )  $\delta$  7.38 – 7.33 (m, 2H), 7.33 – 7.28 (m, 2H), 7.24 – 7.18 (m, 1H), 6.66 (d,  $J = 8.9$  Hz, 2H), 6.50 (d,  $J = 8.9$  Hz, 2H), 5.77 (t,  $J = 6.1$  Hz, 1H), 4.19 (d,  $J = 6.1$  Hz, 2H), 3.78 (t,  $J = 6.5$  Hz, 2H), 1.69 – 1.55 (m, 2H), 1.41 – 1.32 (m, 2H), 1.32 – 1.24 (m, 4H), 0.86 (t,  $J = 7.0$  Hz, 3H).  $^{13}\text{C NMR}$  (125 MHz,  $\text{DMSO-}d_6$ )  $\delta$  150.04, 142.85, 140.55, 128.16, 127.18, 126.47, 115.29, 113.26, 67.84, 47.29, 31.04, 28.88, 25.25, 22.08, 13.89. **IR** ( $\text{cm}^{-1}$ ) 3370, 3000, 2952, 2933, 2870, 2848, 1510, 1475, 1464, 1452, 1406, 1381, 1238, 1028, 823, 700, 744.

**Anal. Calcd. for** C<sub>19</sub>H<sub>25</sub>NO: C, 80.52; H, 8.89; N, 4.94; O, 5.65. Found: C, 80.55; H, 8.83; N, 4.94



**bis(4-methoxyphenyl)amine (16)** In an oven-dried flask palladium acetate (1.80 mmol, 0.40 g, 3% mol) and BINAP (5.40 mmol, 3.36 g, 0.09 eq.) were mixed together with ca. 5 mL of anhydrous toluene under argon and the suspension was allowed to stir for 20 minutes. Then the solution of catalyst was loaded with 4-bromoanisole (66.00 mmol, 12.30 g, 1.10 eq.), 4-methoxyaniline (60.00 mmol, 7.40 g, 1.00 eq.) and sodium *tert*-butanolate (90.00 mmol, 8.65 g, 1.50 eq.). Then it was heated up to 110 °C and stirred overnight. Upon completion the reaction was quenched with water and extracted with diethyl ether. The organic phase was dried with magnesium sulfate and after evaporation of the solvent the crude mixture was chromatographed with hexane/dichloromethane (3/1) mixture to afford the title compound as white solid. 9.22 g yield: 67%.

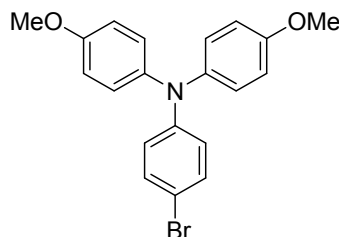
<sup>1</sup>H NMR (400 MHz, DMSO-*d*<sub>6</sub>) δ 7.53 (s, 1H), 6.91 (d, *J* = 9.0 Hz, 4H), 6.80 (d, *J* = 9.0 Hz, 4H), 3.68 (s, 6H). <sup>13</sup>C NMR (100 MHz, DMSO-*d*<sub>6</sub>) δ 152.77, 137.99, 118.00, 114.52, 55.22. IR (cm<sup>-1</sup>) 3423, 3027, 2957, 2935, 2841, 1512, 1512, 1468, 1439, 1299, 1248, 1031, 829, 817. **Anal. Calcd. for** C<sub>14</sub>H<sub>15</sub>NO<sub>2</sub>: C, 73.34; H, 6.59; N, 6.11; O, 13.96. Found: C, 73.29; H, 6.57; N, 6.09.



**4-methoxy-N-(4-methoxyphenyl)-N-phenylaniline (17)** An oven-dried flask was charged with palladium acetate (0.90 mmol, 0.20 g, 3% mol) and tri-*tert*-butylphosphine (2.70 mmol, 0.55 g, 0.09 eq.) in ca. 5 mL of anhydrous toluene under argon and the suspension was allowed to stir for 20 minutes until complete consumption of the solid. Then the solution was loaded with bromobenzene (33.00 mmol, 5.18 g, 1.10 eq.), bis(4-methoxyphenyl)amine (30.00 mmol, 6.88 g, 1.00 eq.) and sodium *tert*-butanolate (45.00 mmol, 4.32 g, 1.50 eq.) in anhydrous toluene (35

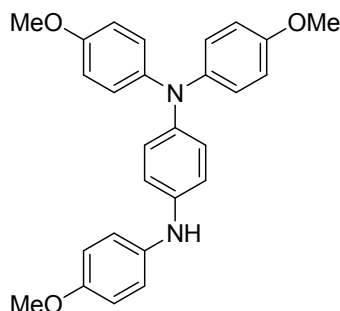
mL). The reaction mixture was then heated to 110 °C and left overnight with stirring. The reaction was ceased with an addition of distilled water and the mixture was extracted with diethyl ether. Upon drying over magnesium sulfate and evaporation of the solvent the crude product was chromatographed with hexane/dichloromethane (2/1) to afford the title compound as white solid. 8.98 g. yield: 98 %.

**<sup>1</sup>H NMR** (400 MHz, DMSO-*d*<sub>6</sub>) δ 7.21 – 7.10 (m, 2H), 6.98 (d, *J* = 9.0 Hz, 4H), 6.89 (d, *J* = 9.0 Hz, 4H), 6.86 – 6.80 (m, 1H), 6.79 – 6.73 (m, 2H), 3.72 (s, 6H). **<sup>13</sup>C NMR** (100 MHz, DMSO-*d*<sub>6</sub>) δ 155.49, 148.37, 140.27, 129.02, 126.36, 120.19, 119.73, 114.86, 55.20. **IR** (cm<sup>-1</sup>) 3033, 2929, 2836, 1592, 1504, 1486, 1467, 1290, 1242, 1032, 834, 700, 758. **Anal. Calcd. for** C<sub>20</sub>H<sub>19</sub>NO<sub>2</sub>: C, 78.66; H, 6.27; N, 4.59; O, 10.48. Found: C, 78.57; H, 6.26; N, 4.61.



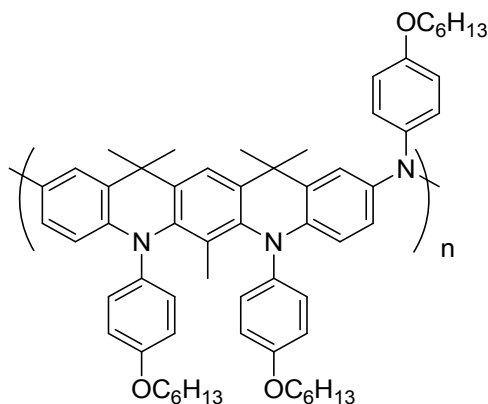
**4-bromo-*N,N*-bis(4-methoxyphenyl)aniline (18)** An oven-dried flask was charged with 4-methoxy-*N*-(4-methoxyphenyl)-*N*-phenylaniline (29.20 mmol, 8.92 g, 1.00 eq.) and diluted with anhydrous DMF (20 mL) under argon. The mixture was cooled to 0 °C and then *N*-bromosuccinimide (32.12 mmol, 5.72 g, 1.10 eq.) in anhydrous DMF (30 mL) was added dropwise over a period of 30 minutes. The solution was brought to room temperature and allowed to stir overnight. Then, it was diluted with distilled water and extracted with diethyl ether. Upon drying over magnesium sulfate and evaporation of the solvent the crude product was chromatographed with hexane/dichloromethane (2/1) to afford a brown oil. It was then further purified *via* crystallization from ethanol, which finally resulted in obtaining the title compound as white solid. 9.65 g. yield: 86%.

**<sup>1</sup>H NMR** (400 MHz, DMSO-*d*<sub>6</sub>) δ 7.30 (d, *J* = 9.0 Hz, 2H), 7.02 (d, *J* = 9.0 Hz, 4H), 6.91 (d, *J* = 9.1 Hz, 4H), 6.66 (d, *J* = 9.0 Hz, 2H), 3.73 (s, 6H). **<sup>13</sup>C NMR** (100 MHz, DMSO-*d*<sub>6</sub>) δ 155.98, 147.82, 139.55, 131.64, 126.88, 120.59, 115.02, 110.83, 55.24. **IR** (cm<sup>-1</sup>) 3037, 2996, 2950, 2832, 1605, 1586, 1503, 1484, 1284, 1238, 1030, 821. **Anal. Calcd. for** C<sub>20</sub>H<sub>18</sub>BrNO<sub>2</sub>: C, 62.51; H, 4.72; Br, 20.79; N, 3.65; O, 8.33. Found: C, 62.43; H, 4.78; N, 3.67.



***N*<sup>1</sup>,*N*<sup>1</sup>,*N*<sup>4</sup>-tris(4-methoxyphenyl)benzene-1,4-diamine (9)** An oven-dried flask was charged with palladium acetate (0.21 mmol, 47 mg, 3% mol) and BINAP (0.63 mmol, 0.39 g, 0.09 eq.) under argon and diluted with ca. 5 mL of anhydrous toluene. The suspension was allowed to stir for 20 minutes and then 4-bromo-*N,N*-bis(4-methoxyphenyl)aniline (7.00 mmol, 2.69 g, 1.00 eq.), 4-methoxyaniline (7.35 mmol, 0.91 g, 1.05 eq.) and sodium *tert*-butanolate (10.5 mmol, 1.01 g, 1.50 eq.) were added. Upon further addition of anhydrous toluene (10 mL) the mixture was heated to 110 °C and stirred overnight. Then it was cooled to room temperature, diluted with water and extracted with diethyl ether. After drying over magnesium sulfate and solvent evaporation the crude product was chromatographed with hexane/ethyl acetate (3/1) to afford yellow oil. The final product was obtained *via* crystallization from hexane as white solid. 2.44 g. Yield: 82%.

**<sup>1</sup>H NMR** (400 MHz, C<sub>6</sub>D<sub>6</sub>) δ 7.14 (d, *J* = 9.1 Hz, 4H), 7.10 (d, *J* = 8.8 Hz, 2H), 6.86 (d, *J* = 9.0 Hz, 2H), 6.75 (d, *J* = 9.0 Hz, 8H), 4.80 (s, 1H), 3.34 (s, 3H), 3.31 (s, 6H). **<sup>13</sup>C NMR** (100 MHz, C<sub>6</sub>D<sub>6</sub>) δ 155.65, 155.34, 142.63, 142.09, 140.29, 137.12, 125.37, 125.26, 121.24, 117.96, 115.05, 115.00, 55.12, 55.07. **IR** (cm<sup>-1</sup>) 3389, 3360, 3032, 2999, 2931, 2827, 1614, 1495, 1462, 1495, 1297, 1232, 1025. **Anal. Calcd. for** C<sub>27</sub>H<sub>26</sub>N<sub>2</sub>O<sub>3</sub>: C, 76.03; H, 6.14; N, 6.57; O, 11.25. Found: C, 75.81; H, 6.09; N, 6.55. **HRMS** (TOF MS ES+) Anal. Calcd. for C<sub>27</sub>H<sub>26</sub>N<sub>2</sub>O<sub>3</sub>: 426.1949 Found: 426.1943 [M<sup>+</sup>].



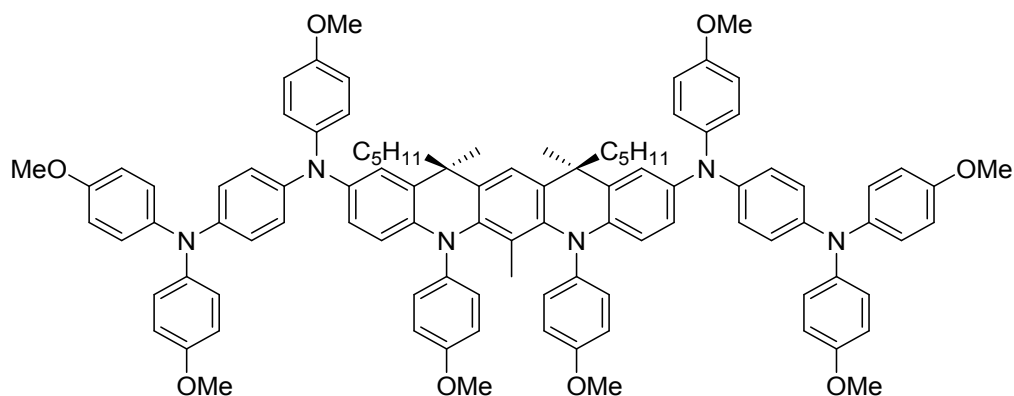
***poly-N,10-(N,5,7-tris(4-(hexyloxy)phenyl)-6,12,12,14,14-pentamethyl-5,7,12,14-tetrahydroquinolino[3,2-*b*]acridin-2-amine) (PQA)***

In an oven-dried schlenk flask were added palladium acetate (0.024 mmol, 6 mg, 2x3% mol), tri-*tert*-butylphosphine (0.072 mmol, 15 mg, 0.18 eq.) and ca. 3 ml of anhydrous toluene under argon. The so-obtained solution was allowed to stir at room temperature for 20 minutes until it turned yellow and then it was charged with 2,10-dibromo-5,7-bis(4-(hexyloxy)phenyl)-6,12,12,14,14-pentamethyl-5,7,12,14-tetrahydroquinolino[3,2-*b*]acridine (0.40 mmol, 0.34 g, 1.00 eq.) and *N*<sup>2</sup>,*N*<sup>10</sup>,5,7-tetrakis(4-(hexyloxy)phenyl)-6,12,12,14,14-pentamethyl-5,7,12,14-tetrahydroquinolino[3,2-*b*]acridine-2,10-diamine (0.40 mmol, 0.43 g, 1.00 eq.). The final solution was the loaded with sodium *tert*-butoxide (1.20 mmol, 0.12 g, 3.00 eq.) and 7 ml of anhydrous toluene. The reaction mixture was degassed by three freeze-pump-thaw cycles and then it was heated to 100 °C and stirred for 5 days. Upon cooling the polymer was precipitated by transfer of the solution into methanol by a pipette. The solid was collected by filtration and then it was washed with hexane to remove the low-molecular weight fractions. The remaining material was dissolved in ca. 3 ml of toluene and methanol was added dropwise to precipitate the high-molecular weight fraction. The precipitate was collected by filtration and vacuum dried to obtain the title polymer as a beige solid. 0.47 g, Yield: 62%.

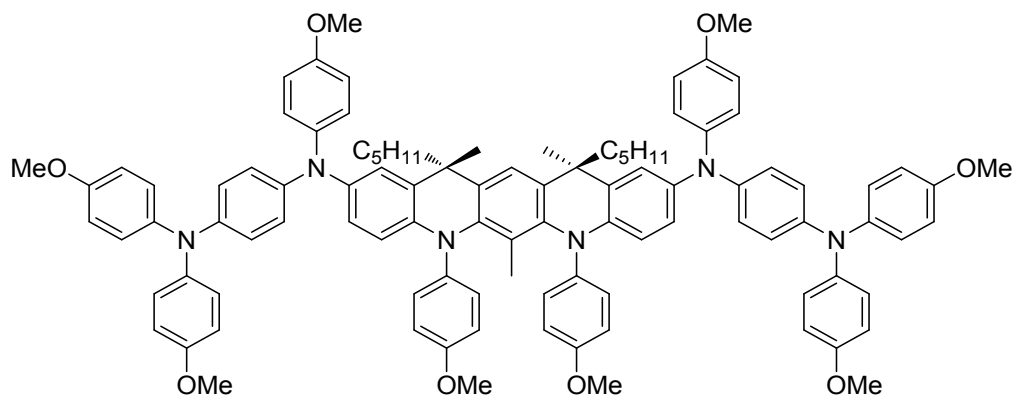
<sup>1</sup>H NMR (500 MHz, THF-*d*<sub>8</sub>) δ 7.44 (d, *J* = 8.5 Hz, 2H), 7.42 (s, 1H), 7.20 (d, *J* = 1.8 Hz, 2H), 7.05 – 6.97 (m, 6H), 6.88 (dd, *J* = 8.5, 1.8 Hz, 2H), 6.80 (d, *J* = 9.0 Hz, 2H), 6.77 (d, *J* = 9.1 Hz, 4H), 3.92 (t, *J* = 6.3 Hz, 2H), 3.88 (t, *J* = 6.3 Hz, 4H), 1.94 (s, 3H), 1.78 – 1.69 (m, 6H), 1.52 – 1.40 (m, 18H), 1.39 – 1.29 (m, 12H), 0.91 (t, *J* = 7.0 Hz, 9H). <sup>13</sup>C NMR (125 MHz, THF-*d*<sub>8</sub>) δ 156.74, 154.74, 145.98, 145.34, 142.07, 141.97, 141.82, 140.28, 139.08, 129.72, 127.45, 127.04, 121.32, 119.65, 118.51, 116.07, 115.63, 68.90, 68.83, 39.17, 32.82, 32.78, 30.62, 30.53, 29.15,

26.97, 26.93, 23.72, 23.71, 15.85, 14.60. IR (KBr,  $\text{cm}^{-1}$ ) 3042, 2953, 2928, 2858, 1604, 1581, 1559, 1506, 1490, 1469, 1459, 1424, 1383, 1361, 1309, 1269, 1239, 1185, 1126, 1098, 1075, 1030, 937, 906, 864, 819, 761, 725, 675, 654, 602, 582, 526. Anal. Calcd. for  $\text{C}_{61}\text{H}_{73}\text{N}_3\text{O}_3$ : C, 81.75; H, 8.21; N, 4.69; O, 5.36. Found: C, 81.60; H, 8.08; N, 4.55. Mn = 161 kDa, Mw = 497 kDa.

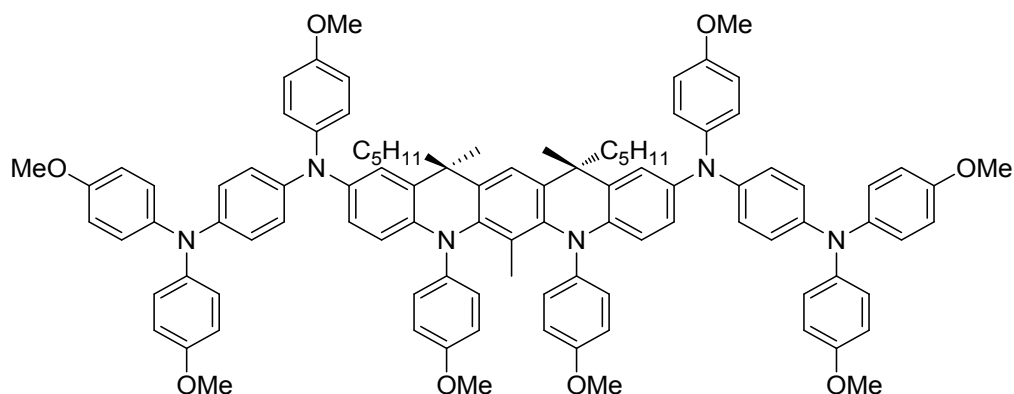
***N*<sup>1</sup>,*N*<sup>1'</sup>-((12*R*,14*S*)-5,7-bis(4-methoxyphenyl)-6,12,14-trimethyl-12,14-dipentyl-5,7,12,14-tetrahydroquinolino[3,2-*b*]acridine-2,10-diyl)bis(*N*<sup>1</sup>,*N*<sup>4</sup>,*N*<sup>4'</sup>-tris(4-methoxyphenyl)benzene-1,4-diamine)**



***N*<sup>1</sup>,*N*<sup>1'</sup>-((12*S*,14*S*)-5,7-bis(4-methoxyphenyl)-6,12,14-trimethyl-12,14-dipentyl-5,7,12,14-tetrahydroquinolino[3,2-*b*]acridine-2,10-diyl)bis(*N*<sup>1</sup>,*N*<sup>4</sup>,*N*<sup>4'</sup>-tris(4-methoxyphenyl)benzene-1,4-diamine)**



***N*<sup>1</sup>,*N*<sup>1'</sup>-((12*R*,14*R*)-5,7-bis(4-methoxyphenyl)-6,12,14-trimethyl-12,14-dipentyl-5,7,12,14-tetrahydroquinolino[3,2-*b*]acridine-2,10-diyl)bis(*N*<sup>1</sup>,*N*<sup>4</sup>,*N*<sup>4'</sup>-tris(4-methoxyphenyl)benzene-1,4-diamine)**



***N*<sup>1</sup>,*N*<sup>1'</sup>-(-5,7-bis(4-methoxyphenyl)-6,12,14-trimethyl-12,14-dipentyl-5,7,12,14-tetrahydroquinolino[3,2-*b*]acridine-2,10-diyl)bis(*N*<sup>1</sup>,*N*<sup>4</sup>,*N*<sup>4</sup>-tris(4-methoxyphenyl)benzene-1,4-diamine)**

**(QA)** An oven-dried flask was charged with palladium acetate (0.078 mmol, 18 mg, 2x3% mol) and tri-*tert*-butylphosphine (0.23 mmol, 47 mg, 0.18 eq.), diluted with anhydrous toluene (ca. 2 mL) under argon. The solution was allowed to stir for 20 minutes and then it was further loaded with

2,10-dibromo-5,7-bis(4-methoxyphenyl)-6,12,14-trimethyl-12,14-dipentyl-5,7,12,14-tetrahydroquinolino[3,2-*b*]acridine (0.36 mmol, 0.30 g, 1.00 eq.), *N*<sup>1</sup>,*N*<sup>1</sup>,*N*<sup>4</sup>-tris(4-methoxyphenyl)benzene-1,4-diamine (0.86 mmol, 0.37 g, 2.40 eq.) and sodium *tert*-butanolate (1.17 mmol, 0.11 g, 3.25 eq.) in anhydrous toluene (8 mL). Then, it was heated to 110 °C and stirred overnight. Upon completion the reaction was quenched with water and extracted with dichloromethane. The organic phase was dried over magnesium sulfate and after evaporation of the solvent the crude solid was chromatographed with hexane/ethyl acetate (3/1). The purified solid was then diluted with ca. 2 mL of THF and precipitated in methanol to afford the final product as greenish-white solid. 0.37 g, yield: 67%.

***N*<sup>1</sup>,*N*<sup>1'</sup>-((12*R*,14*S*)-5,7-bis(4-methoxyphenyl)-6,12,14-trimethyl-12,14-dipentyl-5,7,12,14-tetrahydroquinolino[3,2-*b*]acridine-2,10-diyl)bis(*N*<sup>1</sup>,*N*<sup>4</sup>,*N*<sup>4</sup>-tris(4-methoxyphenyl)benzene-1,4-diamine)**

<sup>1</sup>H NMR (600 MHz, THF-*d*<sub>8</sub>) δ 7.40 (d, *J* = 8.6 Hz, 2H), 7.30 (s, 1H), 7.11 (d, *J* = 2.5 Hz, 2H), 7.05 – 6.93 (m, 16H), 6.91 – 6.84 (m, 6H), 6.84 – 6.75 (m, 20H), 3.74 (s, 6H), 3.73 (s, 12H), 3.71 (s, 6H), 1.86 (s, 3H), 1.65 – 1.52 (m, 10H), 1.18 – 1.00 (m, 8H), 1.00 – 0.90 (m, 4H), 0.72 (t, *J* = 7.3 Hz, 6H). <sup>13</sup>C NMR (150 MHz, THF-*d*<sub>8</sub>) δ 156.93, 156.79, 155.55, 145.68, 144.46, 143.50, 143.29, 142.52, 142.30, 142.22, 142.03, 139.11, 137.55, 128.50, 126.85, 126.52, 126.36,

124.88, 123.69, 121.43, 120.94, 120.88, 119.86, 115.49, 115.47, 114.95, 55.78, 55.75, 55.72, 43.60, 42.54, 33.13, 25.81, 24.57, 23.32, 16.28, 14.54.

*N*<sup>1</sup>,*N*<sup>1'</sup>-((12*R*,14*R*)-5,7-bis(4-methoxyphenyl)-6,12,14-trimethyl-12,14-dipentyl-5,7,12,14-tetrahydroquinolino[3,2-*b*]acridine-2,10-diyl)bis(*N*<sup>1</sup>,*N*<sup>4</sup>,*N*<sup>4'</sup>-tris(4-methoxyphenyl)benzene-1,4-diamine) +  
*N*<sup>1</sup>,*N*<sup>1'</sup>-((12*S*,14*S*)-5,7-bis(4-methoxyphenyl)-6,12,14-trimethyl-12,14-dipentyl-5,7,12,14-tetrahydroquinolino[3,2-*b*]acridine-2,10-diyl)bis(*N*<sup>1</sup>,*N*<sup>4</sup>,*N*<sup>4'</sup>-tris(4-methoxyphenyl)benzene-1,4-diamine)

<sup>1</sup>H NMR (500 MHz, acetone-*d*<sub>6</sub>) δ 7.42 (d, *J* = 8.7 Hz, 2H), 7.39 (s, 1H), 7.13 – 7.08 (m, 2H), 7.05 – 6.96 (m, 16H), 6.91 – 6.77 (m, 26H), 3.74 (s, 6H), 3.73 (s, 12H), 3.71 (s, 6H), 1.77 (s, 3H), 1.74 – 1.62 (m, 4H), 1.54 (s, 6H), 1.14 – 0.92 (m, 12H), 0.68 (t, *J* = 7.0 Hz, 6H). <sup>13</sup>C NMR (125 MHz, acetone-*d*<sub>6</sub>) δ 156.71, 156.55, 155.68, 145.34, 144.36, 142.98, 142.51, 142.23, 142.15, 141.96, 141.52, 139.07, 136.42, 126.87, 126.50, 126.38, 125.66, 124.90, 123.50, 121.62, 121.17, 120.76, 115.49, 114.85, 55.72, 55.69, 42.15, 41.76, 32.80, 28.51, 25.33, 22.95, 16.62, 14.33. IR (cm<sup>-1</sup>) 3033, 2950, 2923, 2833, 1604, 1499, 1462, 1264, 1238, 1036, 824. Anal. Calcd. for C<sub>101</sub>H<sub>102</sub>N<sub>6</sub>O<sub>8</sub>: C, 79.39; H, 6.73; N, 5.50; O, 8.38. Found: C, 79.33; H, 6.73; N, 5.80. HRMS (TOF MS ES<sup>+</sup>) Anal. Calcd. for C<sub>101</sub>H<sub>102</sub>N<sub>6</sub>O<sub>8</sub>: 1526.7749 Found: 1526.7759 [M<sup>+</sup>].

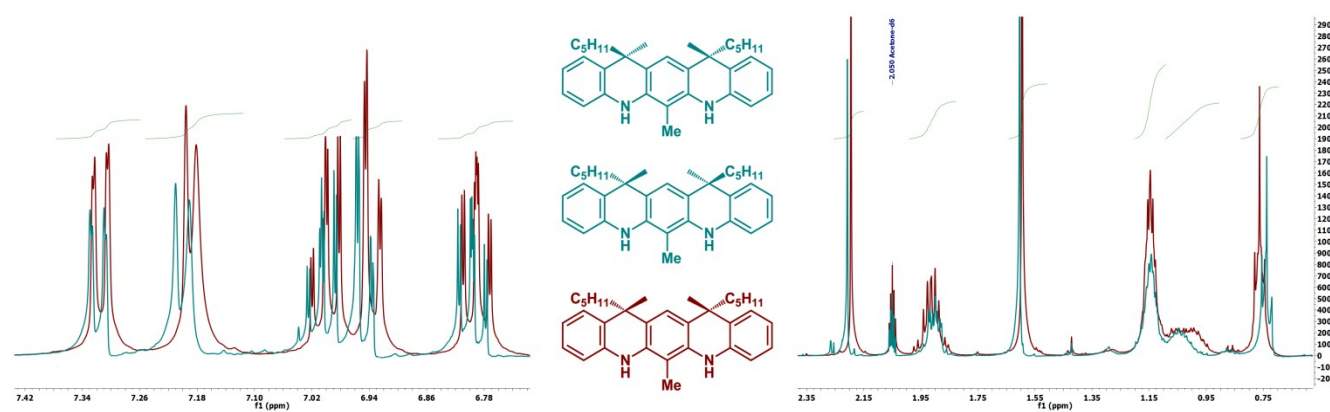


**Figure S1.** The superposition of <sup>1</sup>H NMR spectra of diastereomers of the compound 6b.

### III. Crystallographic Data

Crystal data and structure refinement parameters are given in Table S1. CCDC 1545978 contain supplementary crystallographic data for this paper. These data can be obtained free of charge from The Cambridge Crystallographic Data Centre via [www.ccdc.cam.ac.uk/data\\_request/cif](http://www.ccdc.cam.ac.uk/data_request/cif).

**Table S1.** Crystal data and structure refinement parameters for (12*R*,14*S*)-2,10-dibromo-5,7-bis(4-methoxyphenyl)-6,12,14-trimethyl-12,14-dipentyl-5,7,12,14-tetrahydroquinolino[3,2-*b*]acridine

Empirical formula	C <sub>47</sub> H <sub>52</sub> Br <sub>2</sub> N <sub>2</sub> O <sub>2</sub>
Formula weight	836.72
Temperature [K]	150(2)
Wavelength [Å]	0.71073
Crystal system	Monoclinic
Space group	P2 <sub>1</sub>
Unit cell dimensions	
a [Å]	17.5869(9)
b [Å]	11.4858(6)
c [Å]	20.3691(13)
α	90
β	92.352(5)
γ	90
Volume [Å <sup>3</sup> ]	4111.1(4)
Z	4
Density (calculated) [g/cm <sup>3</sup> ]	1.352
Absorption coefficient [mm <sup>-1</sup> ]	2.012
F(000)	1736
Crystal size [mm]	1.0718 x 0.2363 x 0.0662
θ range for data collection	2.001 to 26.368
Limiting indices	-21 ≤ h ≤ 21 -14 ≤ k ≤ 14 -24 ≤ l ≤ 25
Reflections collected	32117
Independent reflections	16803 [R(int) = 0.0723]
Absorption correction	Analytical
Max. and min. transmission	0.999 and 0.994
Refinement method	Full-matrix least-squares on F <sup>2</sup>
Data / restraints / parameters	16803 / 32 / 987
Goodness-of-fit on F <sup>2</sup>	1.054

Final R indices [ $I > 2\sigma(I)$ ]	R1 = 0.0766, wR2 = 0.1580
R indices (all data)	R1 = 0.1269, wR2 = 0.1851
Absolute structure parameter	0.020(7)
Extinction coefficient	n/a
Largest diff. peak and hole	0.730 and -0.628 e. Å <sup>-3</sup>

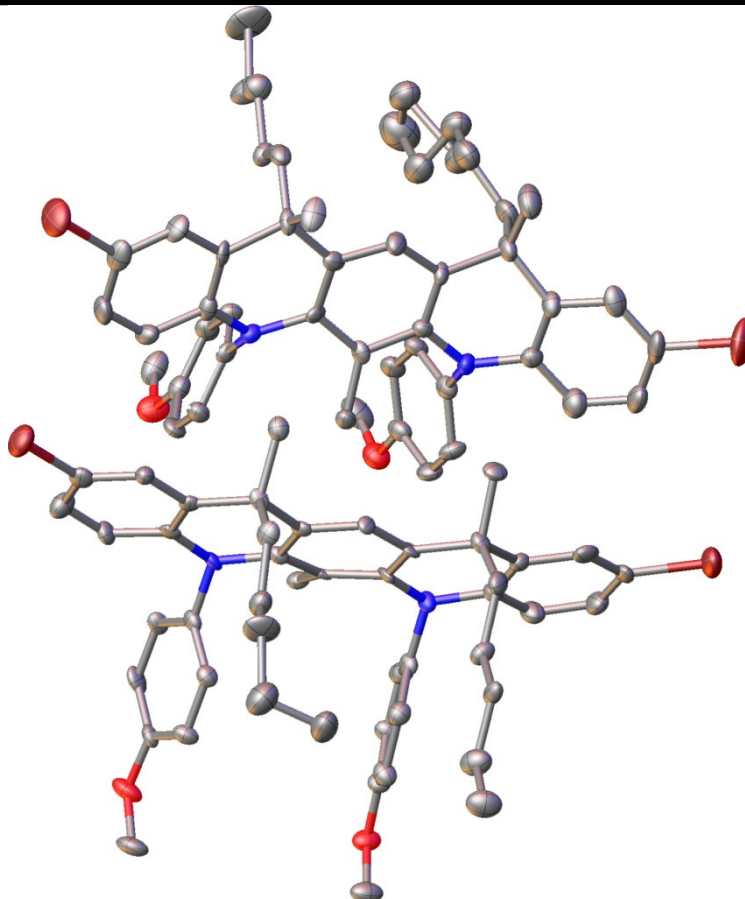


**Figure S2.** The crystal structure of the *meso* form of 8b. Hydrogen atoms have been omitted for clarity.

#### IV. Oxidation Procedure for Pulsed EPR and SQUID Experiments

The chemical oxidation of **QA** and **PQA** was carried out in an argon atmosphere. In a typical procedure 1 ml of 0.015 M solutions of **QA** or **PQA** in dichloromethane were oxidized with the appropriate amount of 0.015 M of tris(4-bromophenyl)ammoniumyl hexachloroantimonate, TBA·SbCl<sub>6</sub> solution in acetonitrile. Then 100 μL of the oxidized solutions were used for pulsed

EPR spectroscopy. For SQUID magnetometry the oxidized solutions were dried under vacuum. The obtained solid-state sample was placed in a Parafilm envelope and inserted in a plastic tube. Diluted QA samples were prepared with 15%<sub>w.t.</sub> of polystyrene solution in CH<sub>2</sub>Cl<sub>2</sub>, mixed with oxidized QA solution and then evaporated under vacuum.

V. The electrochemical oxidation of QA, PQA, D2 and PA2 (CV curves).

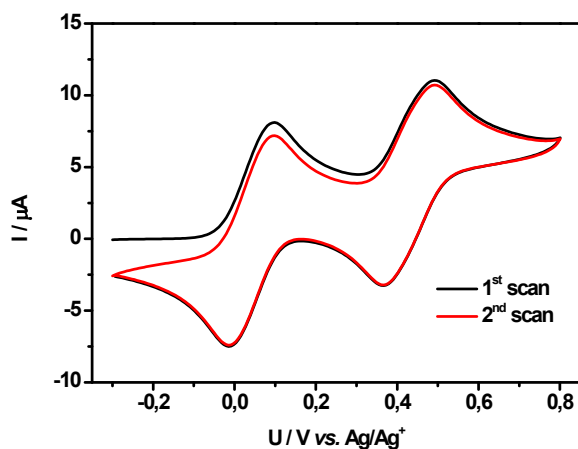


**Figure S3.** Cyclic voltammogram of QA in CH<sub>2</sub>Cl<sub>2</sub> solution (at the concentration  $c = 1 \times 10^{-3}$  M) containing an electrolyte – 0.1 M Bu<sub>4</sub>NBF<sub>4</sub>, (reference electrode – Ag/0.1 M AgNO<sub>3</sub> in acetonitrile, scan rate – 100 mV/s).

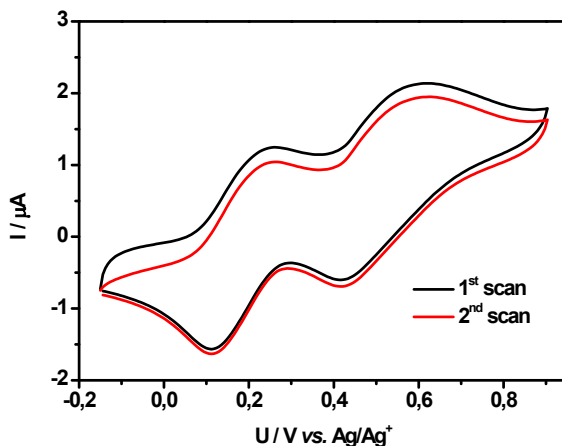


**Figure S4.** Cyclic voltammogram of **PQA** in  $\text{CH}_2\text{Cl}_2$  solution (at the concentration  $c = 1 \times 10^{-3}$  M) containing an electrolyte – 0.1 M  $\text{Bu}_4\text{NBF}_4$ , (reference electrode – Ag/0.1 M  $\text{AgNO}_3$  in acetonitrile, scan rate – 100 mV/s).

## VI. UV-vis-NIR spectra of QA and PQA recorded during chemical oxidation.

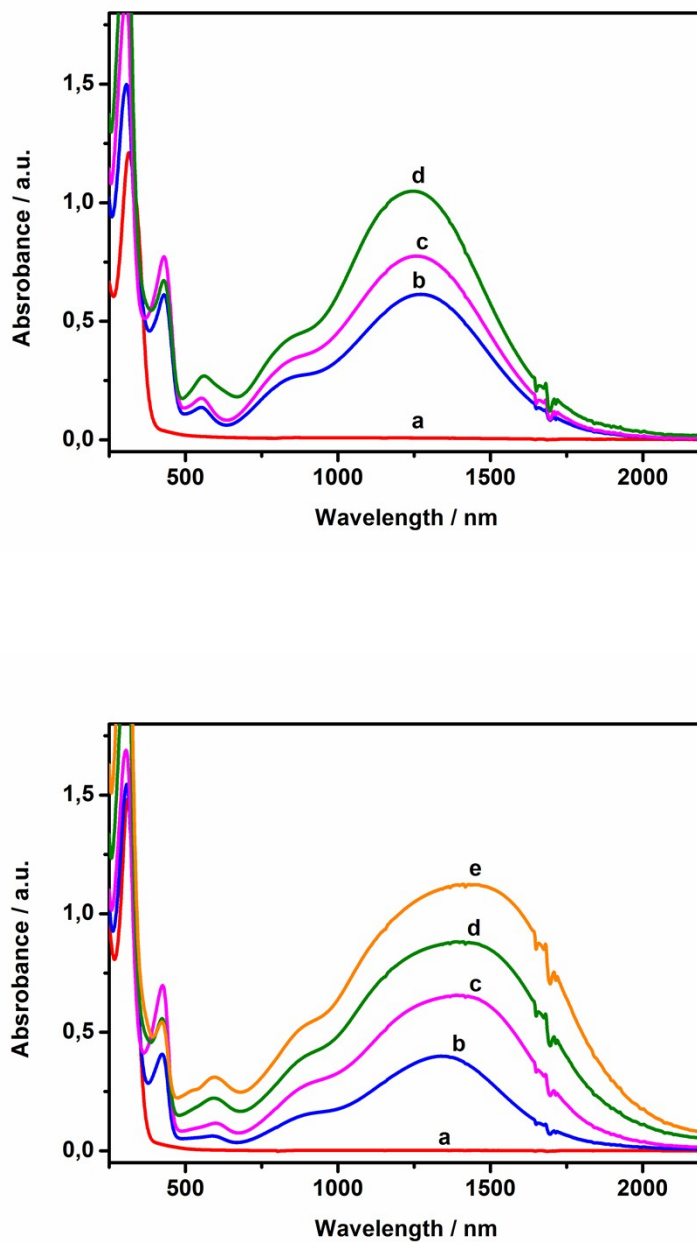


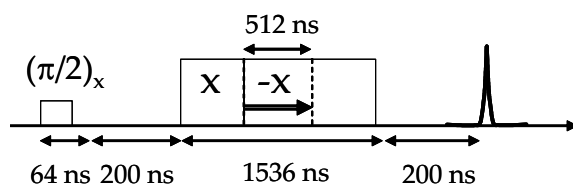
**Figure S5.** The UV-Vis-NIR spectra of **QA** (top) and **PQA** (bottom) oxidized with TBA·SbCl<sub>6</sub> in CH<sub>2</sub>Cl<sub>2</sub>/CH<sub>3</sub>CN solution (the concentration of **QA**  $c = 1.9 \times 10^{-4}$  M, the concentration of **PQA**

$c = 3.8 \times 10^{-4} \text{ M}$ ); the Ox/QA molar ratio: a) 0, b) 1, c) 2, d) 3; the Ox/PQA molar ratio: a) 0, b) 0.5, c) 1, d) 1.5, e) 2.

## VII. Pulsed EPR Nutation Measurements by PEANUT Experiment

Nutation pulsed EPR experiments were performed using a Bruker Elexsys 580 EPR spectrometer in pulsed mode at 7 K. The PEANUT experiment (phase-inverted echo amplitude detected nutation) introduced by Stoll *et al.*<sup>6</sup> was used in order to achieve an optimal resolution of nutation frequencies in the recorded spectra.

The PEANUT experiment is described in **Scheme S3**. In a typical experiment the first pulse used was a selective low power pulse ( $B_1 \sim 0.7 \text{ G}$ ). This pulse was set up to be a true  $\pi/2$  pulse for species having nutation frequencies twice higher than  $S=1/2$  species in order to better detect signals of  $S=3/2$  and  $S=2$  species. Two steps phase cycling ( $+x, -x$ ) was performed on this first pulse. The high turning angle pulses ( $B_1 \sim 7 \text{ G}$ ) had a constant length of 1536 ns and the  $x$  pulse ( $-x$  pulse) was incremented (decremented) by 256 steps of 2 ns, respectively. At every step, the spin rotary echo was integrated using a 76 ns gate centered at its maximum.



**Scheme S3.** Pulses sequence used for the PEANUT experiments.

The obtained time-domain oscillating signal was treated with second order polynomial baseline correction, sinebell transformation and symmetrical zero-filling (256 zeroes added). Then it was Fourier transformed using a numerical FFT software to yield the corresponding nutation spectrum. Two dimensions maps (Magnetic Field vs. Nutation spectrum) were obtained by successively performing PEANUT experiments at 200 magnetic field values spaced by steps of one Gauss.

The spin multiplicities of detected species were obtained by comparing the measured nutation frequency ( $f_{\text{nut}}$ ) to the nutation frequency previously measured for a known  $S=1/2$  systems ( $f_{S=1/2}^{\circ}$ ) and using the following relationship:

$$\nu_{\text{nut}} = \sqrt{S(S+1) - m_s(m_s+1)} \cdot \nu_{S=1/2} \quad (\text{S1})$$

This relationship is given for an EPR  $|S, m_s\rangle \longleftrightarrow |S, m_s+1\rangle$  transition and is valid for low magnetic field excitation ( $B1 \ll D$ ,  $D$  the axial zero field splitting parameter of the considered species).<sup>7</sup>

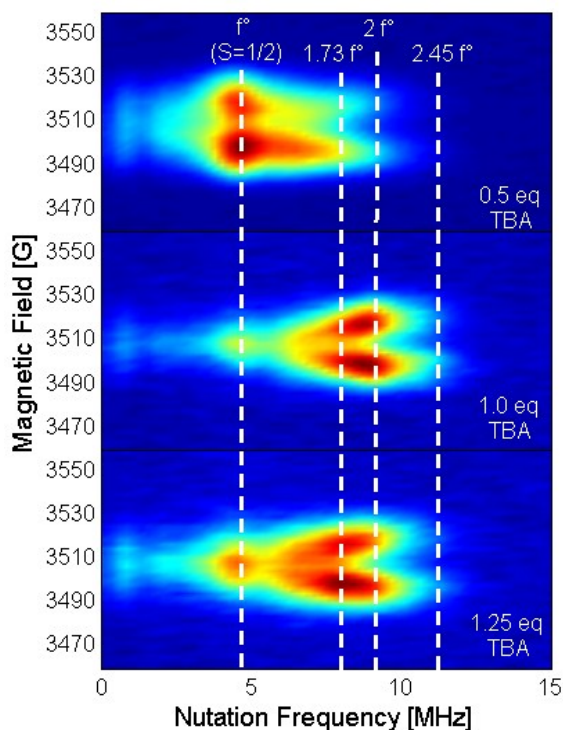


**Figure S6.** 2D field swept pulsed-EPR nutation spectra of **PQA** ( $T=7\text{K}$ ). PQA samples were oxidized with  $\text{TBA}\cdot\text{SbCl}_6$  in  $\text{CH}_2\text{Cl}_2/\text{CH}_3\text{CN}$  solution ( $[\text{PQA}] = 7.5 \cdot 10^{-3} \text{ M}$  and  $[\text{TBA}]/[\text{PQA}] = 0.5, 1$  and  $1.25$  for upper, middle and lower spectra respectively). In this experiments the microwave pulse power is set so that the nutation frequency for  $S=1/2$  is  $f^{\circ} = 4.4 \text{ MHz}$ .

The pulsed-EPR nutation spectra of PQA oxidized by various amounts of TBA·SbCl<sub>6</sub> is shown in **Figure S6**. In the conditions of the experiments reported in **Figure S6**, S=1/2 species are expected at  $\nu_0=4.4$  MHz nutation frequency. Accordingly, the following nutation frequencies are expected for higher spin states:

- i) for S=1,  $f_{(S=1)}=\sqrt{2}\cdot f^\circ=6.2$  MHz,
- ii) for S=3/2,  $f_{\text{nut}}=\sqrt{3}\cdot f^\circ=7.6$  MHz (for the  $|3/2,1/2\rangle \leftrightarrow |3/2,3/2\rangle$  and the  $|3/2,-3/2\rangle \leftrightarrow |3/2,-1/2\rangle$  EPR transitions) and  $f_{\text{nut}}=2\cdot f^\circ=8.8$  MHz (for the  $|3/2,-1/2\rangle \leftrightarrow |3/2,1/2\rangle$  EPR transition),
- iii) for S=2,  $f_{\text{nut}}=2\cdot f^\circ=8.8$  MHz (for the  $|2,-2\rangle \leftrightarrow |2,-1\rangle$  and the  $|2,1\rangle \leftrightarrow |2,2\rangle$  EPR transitions) and  $f_{\text{nut}}=\sqrt{6}\cdot f^\circ=10.8$  MHz ( $|2,-1\rangle \leftrightarrow |2,0\rangle$  and the  $|2,0\rangle \leftrightarrow |2,1\rangle$  EPR transitions).

These frequencies are indicated by white lines in the spectra reported in the **Figure S9**.

For the sample with [TBA]/[PQA]=0.5, a dominant S=1/2 state is observed and weaker signals corresponding to higher S=1 and S=3/2 spin states are also observed. For the sample with [TBA]/[PQA]=1.0, the dominant signal has a nutation frequency close to  $2\cdot f^\circ$  and a small but clear signals can be observed up to  $\sqrt{6}\cdot f^\circ$ . Such a spectrum is typical of S=2 spin states and demonstrates that S=2 states are dominant in stoichiometrically oxidized PQA. For the sample with [TBA]/[PQA]=1.25, the dominant signal is maximal for a nutation frequency close to  $\sqrt{3}\cdot f^\circ$ , indicating that most species are in the S=3/2 state and signals at higher frequencies are lower, indicating that S=2 states are in smaller amount than in the sample doped with the best stoichiometry ([TBA]/[PQA]=1.0). From these experiments, one can conclude that the best oxidation stoichiometry for obtaining high spin states from PQA is [TBA]/[PQA]=1.0, and that this results in a S=2 spin state.

## VIII. SQUID Magnetometry

### Magnetization measurements mode

For magnetization measurements the solutions of the oxidized QA and PQA were evaporated and pumped under a vacuum for 0.5 h. The solid-state samples thus obtained were placed under a protective argon atmosphere in Parafilm envelopes (showing a controlled diamagnetic signal)

and transferred to the magnetometer. Magnetization of the samples was measured as a function of magnetic field (up to 7 T) and temperature ( $2 \text{ K} < T < 275 \text{ K}$ ) using a superconducting quantum interference device (SQUID) magnetometer.

The sequence of the measurements was following:

- i) the sample was cooled to 2 K and the magnetization was measured vs. magnetic field for  $T=\text{const.}$  (at  $T= 2, 5, 10$  and  $30 \text{ K}$ ),
- ii) the sample was cooled again to 2 K and magnetization vs.  $T$  was measured for  $B=1 \text{ T}$  (temperature range  $2 - 275 \text{ K}$ ); the heating rate was changed at  $10 \text{ K}$  and  $50 \text{ K}$ ,
- iii) magnetization was measured vs.  $B$  for  $T=275 \text{ K}, 200 \text{ K}, 100 \text{ K}$  and  $50 \text{ K}$ ,
- iv) the sample was cooled to 2 K and magnetization measurements vs.  $T$  were repeated for  $B=0.5 \text{ T}$ .

The magnetization data were corrected for diamagnetism of the Parafilm envelopes and the samples themselves (extrapolated from high-temperature magnetization data).

### Magnetic properties studies

Both samples **QA** and **PQA** show typical Brillouin-type behavior: at low temperatures magnetization tends to saturate with magnetic field  $B$ , while at higher temperatures it is almost linear with  $B$  and decreases with increasing temperature. Typical results of magnetization of **QA** dimer as a function of magnetic field at different temperatures are shown in Figure S7.

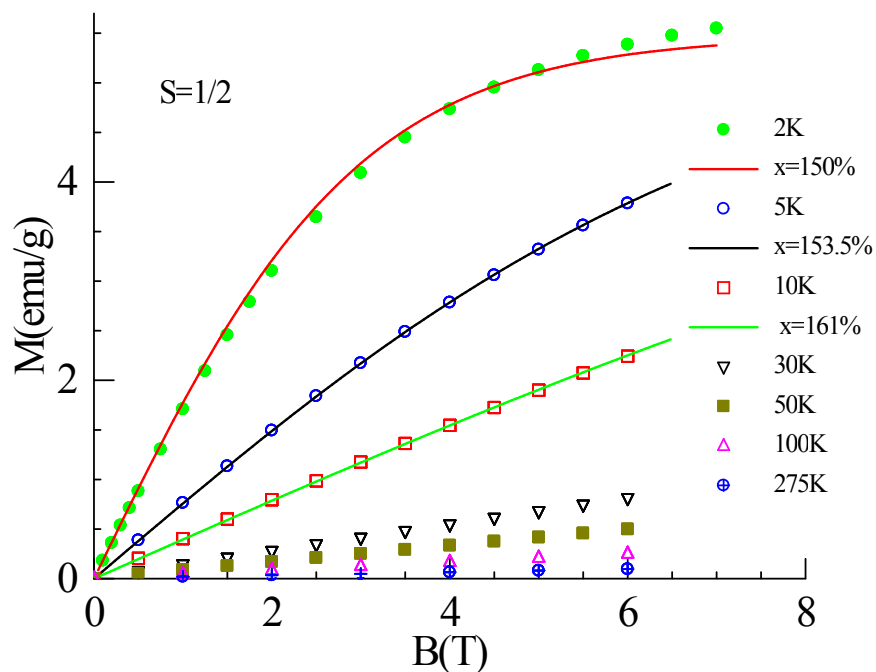


**Figure S7.** Magnetization of QA versus magnetic field at different temperatures.

Non-interacting unpaired electrons of radical cations should be the source of magnetic moments with  $S=1/2$  and can be described by a standard Brillouin function in the following way:

$$M(B,T) = N \cdot x \cdot g \cdot \mu_B \cdot S \cdot B_S(B,T) \quad (S2)$$

where  $B_S(B,T)$  denotes the Brillouin function for spin  $S$ ,  $N$  is the number of molecules per mass unit,  $g$  is  $g$ -factor and  $\mu_B$  denotes Bohr magneton. The spin concentration  $x$  is expressed as a number of radical cations per molecule. Figure S7 shows that experimental data can be well fitted with the Brillouin function for  $S=1/2$  (the three solid lines in Fig. S7). The only adjustable parameter was the radical cations concentration,  $x$ . One can observe that the spin concentration highly exceeded 100%, thus a large number of molecules contained two spins  $S=1/2$ . The concentration of spins per molecule increased slightly with increasing temperature from *ca.* 150% at the lowest temperature ( $T=2$  K, however the experimental points were not perfectly

fitted with the Brillouin function in this case) to 153.5% at 5 K and 161% at 10 K. This behavior will be discussed further. For this reason one should expect that *ca.* 87% to 58% of **QA** molecules contained two spins which can interact ferromagnetically *via meta*-phenylene coupler. This assumption was consistent with the results of pulsed-EPR study which showed that spins interact and form the triplet state  $S=1$ .

The low temperature magnetization of interacting spins system is commonly described by the effective Brillouin function.<sup>8</sup> Possible interactions between molecules can be taken into account by assuming effective temperature  $T_{\text{eff}} = T - \theta$ , instead of experimental temperature  $T$ , with  $\theta$  being an adjustable parameter. In the case of ferromagnetic interaction (FM) between spins magnetization saturates faster than the simple Brillouin function, which corresponds to an effective temperature lower than the experimental  $T$ , so  $\theta > 0$ . On the other hand for antiferromagnetically (AFM) coupled spins the situation is reversed (*i.e.*  $\theta < 0$ ). Figure S8 shows the experimental data measured at 2 K which can be approximated with three curves by modifying three parameters, *i.e.* the  $S$  value, the spin concentration  $x$  and the effective temperature  $\theta$ . Fitting magnetization data with the effective Brillouin function with fixed  $S=1$  returned  $\theta = -0.925 \text{ K} < 0$  and  $x=78\%$ . If one can take into account the presence of some molecules with only one unpaired electron ( $S=1/2$ ), thus the  $S$  value should be lower than 1 with simultaneous increase of spin concentration  $x$  (for example for  $S=0.878$ ,  $x=89\%$ ).

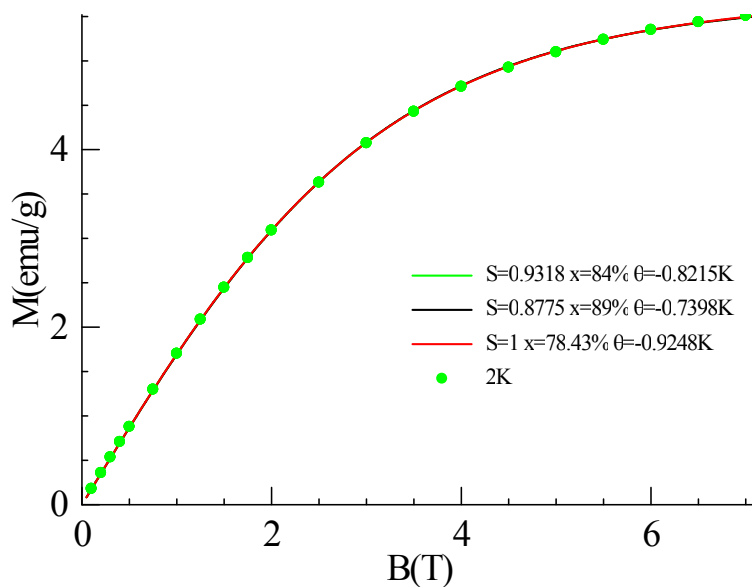


**Figure S8.** Magnetization of **QA** versus magnetic field at  $T=2$  K approximated with the effective Brillouin function for  $S \approx 1$ .

It should be emphasized that the parameter  $\theta$  reflects antiferromagnetic intermolecular coupling and cannot be negligible for solid state samples. All above approximations show that *ca.* 80-85% of **QA** molecules could contain two interacting spins which form triplet state  $S=1$  (evidenced also in EPR studies).

The best way to demonstrate existing interactions between magnetic centers is to plot the product of the magnetization and temperature  $MT$  vs. temperature  $T$ . For a purely paramagnetic and non-interacting system of magnetic moments  $MT$  does not depend of  $T$  at not very low temperature range ( $T \geq 6$  K for  $B=1$  T, see blue line Fig. S9). Moreover, the constant value of  $MT$  is related with the number of magnetic centers in the system. On the other hand, the interactions in the paramagnetic phase result in  $MT$  deviation from constant value: downward in the case of AFM interactions and upward for the FM interactions. The downward slope is, therefore, recognized as a signature of the interactions among magnetic centers in the paramagnetic phase which is equivalent to freezing out some spins by antiferromagnetic coupling.

The magnetization measurements versus temperature at  $B=1$  T of the solid state sample **QA** is shown in Figure S9.

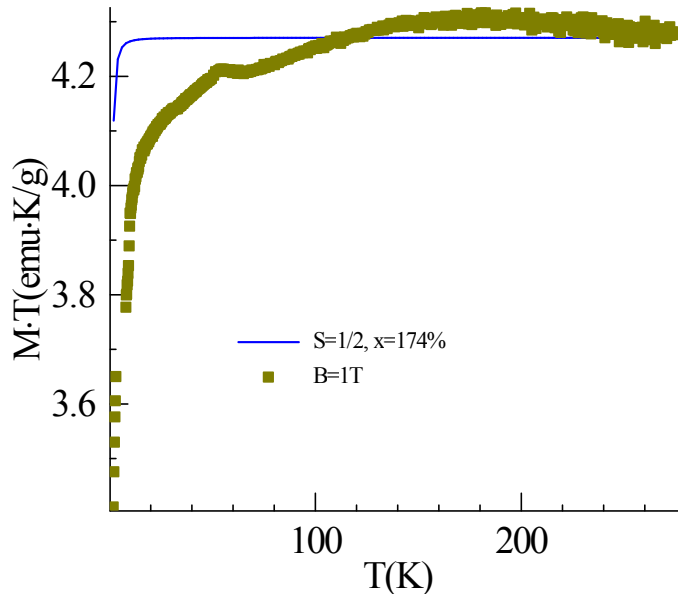


**Figure S9.** Product of magnetization and temperature ( $M \cdot T$ ) vs. temperature at  $B=1$  T. Blue line represents the Brillouin function fit for non-interacting spins  $S=1/2$  and  $x=174\%$ .

The above curve increases slightly with decreasing temperatures from 275 K to *ca.* 160 K, then falls down with decreasing temperature towards the low value. The observed increase of  $MT$  results from ferromagnetic intramolecular interaction of two spins in the molecule coupled *via meta*-phenylene ring, while subsequent drop of  $MT$  value reflects antiferromagnetic intermolecular interaction. It can be due to co-planar nature of **QA** molecules which in solid state are closely packed, thus the intermolecular antiferromagnetic character dominates. To avoid the problem of intermolecular antiferromagnetic interactions **QA** samples were diluted in polystyrene matrix. However, for this type of samples the paramagnetic contribution (PM) was dramatically decreased in comparison to the diamagnetic one, especially in the high temperature range. This in turn results in underestimated value of PM contribution\*. Figure S10 and Figure 4a of the main text show the results of magnetization of **QA** dimer diluted in polystyrene matrix (8%<sub>wt.</sub>, *i.e.* 0.58%<sub>mol.</sub> of **QA** in polystyrene) as a function of magnetic field at  $T=2$  K.

\*(the small mass of QA in comparison to total mass hampers its homogenous distribution in the sample, it means that paramagnetic and diamagnetic parts were not good centered. So, the paramagnetic contribution was underestimated, especially at high temperatures)

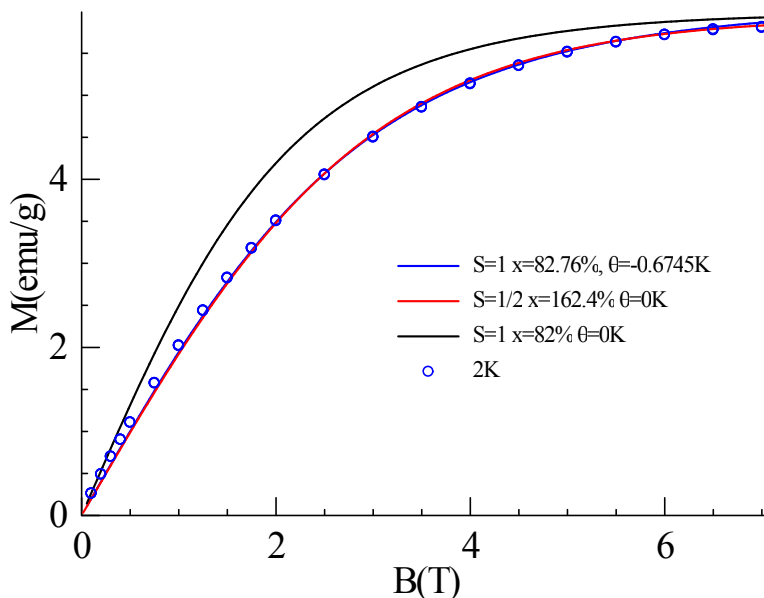


**Figure S10.** Magnetization of QA diluted in polystyrene matrix (0.58%<sub>mol.</sub>) versus magnetic field at  $T=2$  K (the red and blue curves overlap).

The experimental data can be very well fitted using the effective Brillouin function for  $S=1$  with  $x$  equal to *ca.* 82% and  $\theta = -0.6745$  K. It should be emphasized that the concentration of spins for this sample is comparable to that obtained for solid state sample. The smaller value of  $\theta$  than determined for solid state sample indicates weaker antiferromagnetic interaction after the separation of QA molecules in polymer matrix. The product of magnetic susceptibility and temperature ( $\chi T$ ) vs. temperature at  $B=0.5$  T is shown below in Figure S11 and Figure 4b of the main text.

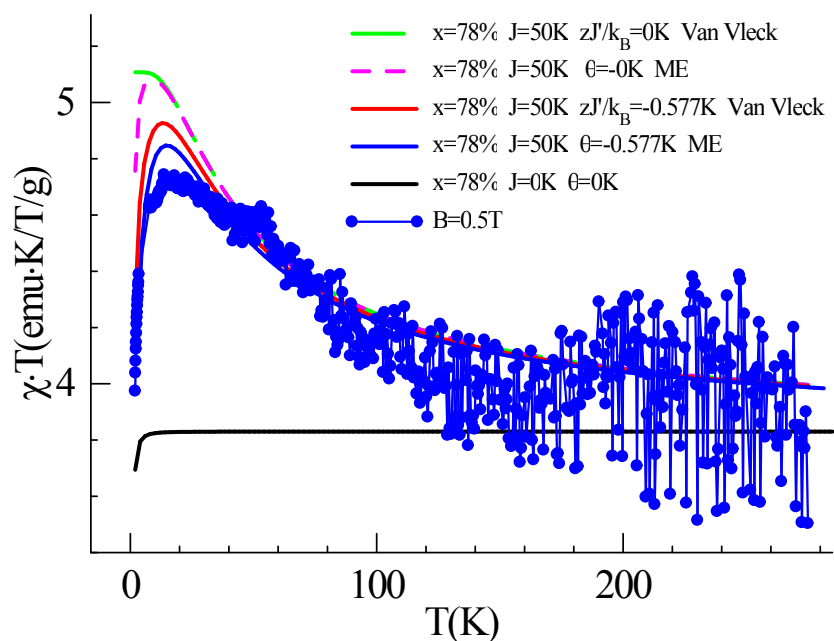


**Figure S11.** Product of magnetic susceptibility and temperature ( $\chi T$ ) vs. temperature at  $B=0.5$  T obtained for **QA** sample diluted in polystyrene matrix.

The curve shown in Figure S11 exhibits quite different character than that presented in Figure S9, namely  $\chi T$  starts to increase with decreasing temperature from  $T \approx 150$  K to *ca.* 20 K, then falls down for lower temperatures. Thus, in the 20 - 275 K temperature range the ferromagnetic intramolecular interactions between spins in **QA** dimer are dominant. Below 20 K the curve drops down indicating antiferromagnetic intermolecular interaction, which is typical for this type of compounds. However, due to the dilution the paramagnetic contribution of **QA** was very weak at high temperatures range. PM contribution could not be accurately determined by the correction procedure as noted above. Nevertheless, to analyze further the experimental data it would be interesting to apply the two approximate formulas.

Firstly, since we treat the case of weak intermolecular interactions ( $zJ$ ) superimpose on the dominant intramolecular interaction ( $J$ ) in biradical compounds and we can adopt the equation based on Van Vleck approximation. It was successfully used to a few copper(II) dinuclear compounds with a triplet ground state ( $J > 0$ ) showing weak antiferromagnetic intermolecular interaction ( $zJ < 0$ ).<sup>9</sup> The equation reads:

$$\chi T = 2Ng^2\mu_B^2T \left[ k_B T - \frac{2zJ}{3 + \exp\left(-\frac{J}{k_B T}\right)} \right]^{-1} \left[ 3 + \exp\left(-\frac{J}{k_B T}\right) \right]^{-1} \quad (\text{S3})$$

where:  $z$  is the number of nearest neighbors, which is not known in our case, so we use the product  $zJ$  as a parameter.

Secondly, we use the fact that for two interacting electrons (described by Heisenberg exchange –  $JS_1S_2$ ) we have the strict equation:

$$M(B,T) = Ng\mu_B \frac{2\sinh\left(\frac{g\mu_B B}{k_B T}\right)}{\exp\left(-\frac{J}{k_B T}\right) + 2\cosh\left(\frac{g\mu_B B}{k_B T}\right) + 1} \quad (\text{S4})$$

Taking into account possible intermolecular interactions we use, as before, the concept of the effective temperature ( $T - \theta \rightarrow T$ ).

From the Figure S11 (Figure 4b of the main text) of the main text is readily seen that the experimental data can be approximated using Van Vleck equation (S3) or the magnetization equation (ME) (S4) with an effective temperature  $\theta$ . Both equations led to similar value of the exchange coupling constant  $J/k_B=50$  K for 78% of **QA** molecules containing triplets which is in agreement with the number of **QA** molecules found from the fit to the  $M$  vs.  $B$  at  $T=2$  K data (Figure S10). However, taking into account large noises \* of the curve  $\chi T$  vs.  $T$ , this approximation leads to rather qualitative not quantitative conclusion and the  $J$  value is rather estimated than determined.

Magnetization measurements were performed also for the polymer **PQA**. Typical results of magnetization of solid state sample of **PQA** as a function of magnetic field at different temperatures and the product of magnetic susceptibility and temperature versus temperature are

shown in the manuscript (Fig. 5). The experimental data were described by the model calculations using Heisenberg exchange Hamiltonian.

If there is no intermolecular interaction in the system the magnetization can be calculated exactly.

<sup>10</sup> Assuming that intramolecular interactions can be described by a Heisenberg exchange the Hamiltonian for a single chain segment with four interacting spins  $S=1/2$  can be written in the form:

$$H = (-J \cdot S_1 S_2 - J \cdot S_2 S_3 - J \cdot S_3 S_4) + \mu_B (2S_1 + 2S_2 + 2S_3 + 2S_4) B \quad (S5)$$

where: the first term corresponds to a Heisenberg exchange and the second one is the Zeeman term. Numerical solution of the Hamiltonian allows one to determine eigenstates and magnetization  $M$  and then calculate the product of  $M \cdot T$  vs.  $T$ . Finally, taking into account the intermolecular interaction, similarly as in the case of **QA**, the concept of the effective temperature ( $T - \theta \rightarrow T$ ) was applied.

## IX. DFT Methodology

All DFT calculations have been performed with the ADF (Amsterdam Density Functional) 2013.01 code developed by Baerends *et al.*<sup>11</sup> Triple-*zeta* basis sets (with the “no core” option activated) have been used throughout for all atoms. We relied on the VBP (Vosko, Wilk, and Nusair)<sup>12</sup> exchange-correlation (XC) potential (completed by nonlocal gradient corrections to the exchange by Becke<sup>13</sup> as well as to the correlation by Perdew<sup>14</sup>) for geometry optimizations (due to the size of most of the molecules: 193 atoms for the biggest QA model) and computation of orbitals for mono-oxidized states (to amplify the localization/delocalization effect for illustrative purpose: see below). We further used B3LYP<sup>15,16</sup> exchange-correlation (XC) potential mixing in 20% of Hartree-Fock true exchange within the DFT XC potential for the computation of exchange coupling constants  $J$  (with  $\mathbf{H} = JS_1 \cdot S_2$ ) relying on the Broken Symmetry methodology developed originally by L. Noodleman<sup>17-20</sup>.

### 1°) Molecular orbital shapes for the mono-oxidized state.

We show experimentally that, in terms of redox potentials, the use of the planar 5,7,12,14-tetrahydroquinolino[3,2-*b*]acridine core for both **QA** and **PQA** almost cancels the cost of oxidizing two arylamines connected by the *m*-phenyl spin coupler. In the case of the dimer **QA** for example, for the second oxidation to occur at about the same potential as the first one implies that the unpaired electron resulting from the first oxidation (or equivalently the corresponding hole) is more localized/lateralized than in **D2** for which the second oxidation occurs at a non-negligible cost (~85 mV shift). To hint at a possible theoretical explanation of such a differential effect between **D2** and **QA**, we computed electronic structures for *mono-oxidized* states for both **D2** and a QA-model derived from **D2** by only adding the rigidifying CH<sub>2</sub> bridges (hence **QA<sub>D2</sub>**).

When one computes *in vacuo* the HOMOs resulting from the first oxidation for both **D2** and **QA<sub>D2</sub>**, they are both for symmetry reasons artificially delocalized over the dimers (see Figure 12). Obviously, the real environment of these dimers is not isotropic (as it is *in vacuo* or in a polarizable dielectric medium). As it turns out, the differential behavior of **D2** versus **QA<sub>D2</sub>** is revealed in the presence of a lateral charge (modeling the counter-anion). We namely placed a negative charge above the central nitrogen of one of the spin bearers, perpendicular to its local plane and at a distance of 3 Å (via the ADF option: Efield). It is then remarkable to observe that, even for a fractional negative charge ( $q = -0.25 e^-$  in Figure S13), the HOMO of **QA<sub>D2</sub>** become fully localized/lateralized whereas that of **D2** is only partially lateralized for the same charge placed at the same place (only results for  $q = -0.25 e^-$  are here shown, but calculations have been performed for  $0 \leq |q| \leq 1$  by step of 0.25). The idea suggested by these preliminary DFT calculations is the following: the expected lateralization of the HOMO enforced by an anisotropic environment (*i.e.* counter-anion nearby) statistically allows for a second oxidation of **QA<sub>D2</sub>** at nearly no cost whereas such is not the case for **D2** due to the leakage of the HOMO onto the other side of the dimer.

The way orbital ( $\pi$ ) conjugation/spin alternation operate in these aromatic compounds seems to play a significant role in this differential effect. Spin alternation is enforced in **QA<sub>D2</sub>** because of the local planarity of the dimer around the central *meta* spin coupler whereas the breaking of that planar symmetry in the case of **D2** is the cause of the charge leakage mentioned above. To illustrate that point, we also computed the HOMO of the *mono-oxidized* state for a dimer derived

from  $\text{QA}_{\text{D2}}$  by changing the central *meta*-coupler into a *para*-coupler, thus inverting spin alternation around the coupler. This **paraQA<sub>D2</sub>** (for lack of a better name) was fully geometry-optimized (VBP level) and a lateral charge ( $-0.25 e^-$ ) was placed at the same relative position as for  $\text{QA}_{\text{D2}}$  and **D2**. As can be seen in Figure S14, no lateralization occurs at all.

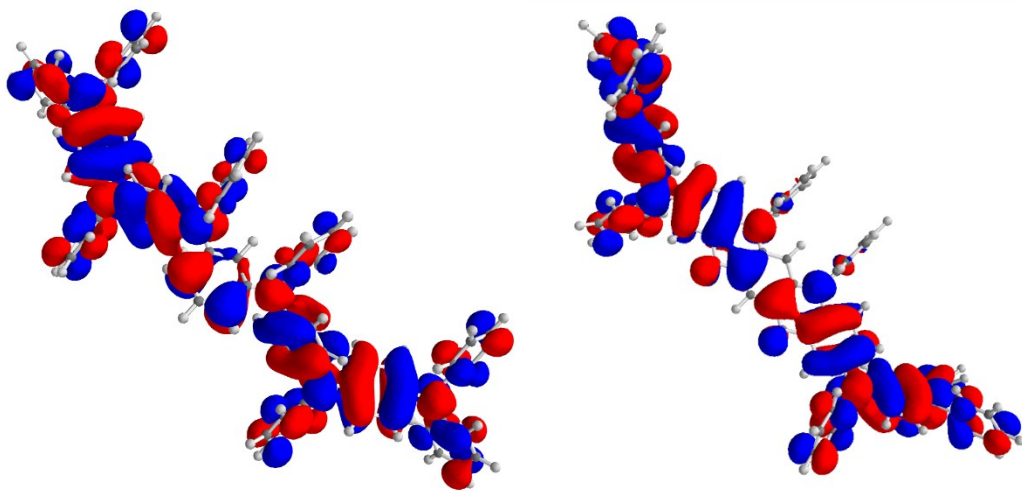


**Figure S12.** HOMOs in the *mono-oxidized* states of **D2** (left) versus  $\text{QA}_{\text{D2}}$  (right) without lateral charge breaking the isotropic symmetry of the environment. Isodensity value = 0.01 a.u.

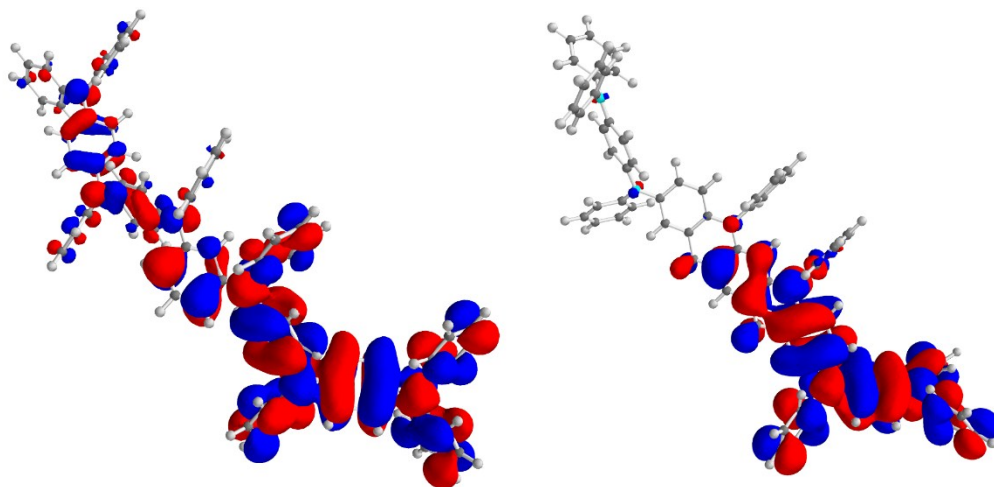


**Figure S13.** HOMOs in the *mono-oxidized* state of **D2** (left) versus  $\text{QA}_{\text{D2}}$  (right) in the presence of a lateral ( $-0.25 e^-$ ) charge. Isodensity value = 0.01 a.u.

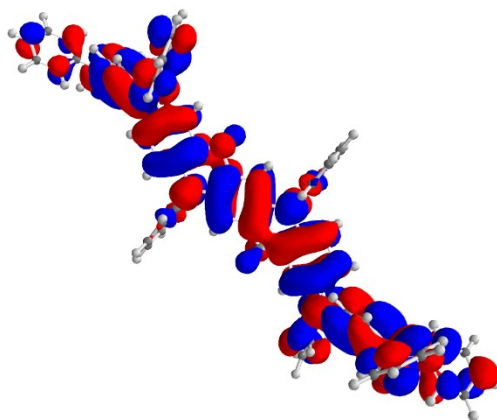


**Figure S14.** HOMOs in the *mono-oxidized* state of **paraQA<sub>D2</sub>** (notice the trans-positions of the two pending phenyl groups) in the presence of a lateral ( $-0.25 e^-$ ) charge. Isodensity value = 0.01 a.u.

## 2°) Exchange coupling constants $J$

For comparison purposes,  $J/k$  values have been first computed for **QA<sub>D2</sub>** derived from **D2** by only adding the rigidifying  $\text{CH}_2$  bridges (cf. 1°). Furthermore, simplified versions of **D2** and **QA<sub>D2</sub>** have been considered in which all pendant phenyl groups have been replaced by hydrogens (**D2<sub>H</sub>** versus **QA<sub>D2-H</sub>**). As can be seen in Table S2, the impact of introducing the  $\text{CH}_2$  bridges on  $J$  values is significant. Comparing the “real” **D2** with **QA<sub>D2</sub>** (*i.e.* both with pendant phenyl groups), the gain is of a factor 3.5 which lead us to high expectations for the experimental **QA** dimer ... till we computed  $J/k$  for **QA** (see below).

**Table S2.** DFT computed  $J/k$  values (in Kelvin) for **D2** and **QA** models (see description of the models in the main ESI text).

$J/k$ (K)	<b>D2<sub>X</sub></b>	<b>QA<sub>D2-X</sub></b>	Ratio $J/k(\text{QA}_{\text{D2-X}})/J/k(\text{D2}_X)$
<b>X = blank</b>	35	116	3.5
<b>X = H</b>	88	165	1.9

Next, and in order to understand better the various contributions of **QA** features (*i.e.* pendant phenyl groups, donor OMe groups, CH<sub>2</sub> versus more donor CMe<sub>2</sub> bridges, etc.) to the value of the exchange coupling constant  $J$ , we considered four models for **QA** of increasing complexity (*i.e.* coming each time closer to the experimental **QA** dimer).

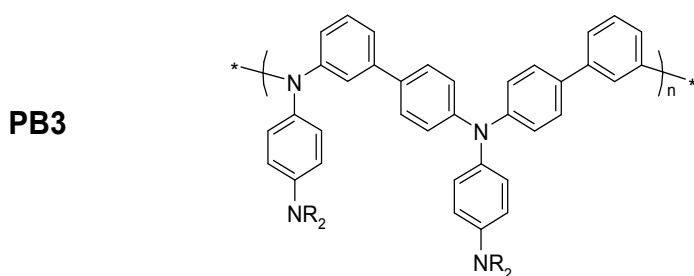
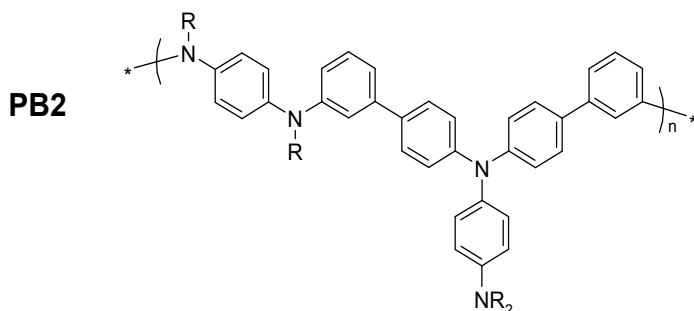
The first two models are the one we proposed above, that is **QA<sub>D2-H</sub>** (with CH<sub>2</sub> bridges but no pending phenyl groups) and **QA<sub>D2</sub>** (with CH<sub>2</sub> bridges and pending phenyl groups). To the third QA model, **QA<sub>OMe</sub>**, we add the donor OMe moieties to the phenyl groups to the previous **QA<sub>D2</sub>**. Finally, we considered a quasi-**QA** dimer, with CMe<sub>2</sub> bridges (**QA<sub>CMe</sub>**). Bonding energies for HS (triplet) and BS (Ms=0) states, as well as resulting  $J/k$  values are reported in **Table S3**.

**Table S3.** DFT computed bonding energies (eV; B3LYP) for HS (S=1) and BS (Ms=0) states, and resulting  $J/k$  values (in Kelvin) for **D2** and **QA** models (see description of the models in the main ESI text).

<b>Energies</b>	<b>QA<sub>D2-H</sub></b>	<b>QA<sub>D2</sub></b>	<b>QA<sub>OMe</sub></b>	<b>QA<sub>CMe</sub></b>
<b>E<sub>HS</sub> (eV)</b>	-483.822	-1095.764	-1306.540	-1399.792
<b>E<sub>BS</sub> (eV)</b>	-483.815	-1095.759	-1306.537	-1399.790
<b>J/k(DFT) (K)</b>	165	116	81	42

First, our DFT calculations reproduce well the experimental value ( $J/k = 50$  K) for the QA model designed to be the closest one to the actual **QA** dimer, *i.e.* **QA<sub>CMe</sub>** (42 K in **Table S3**). We see however how tending towards more realistic models, starting from the simplest **QA<sub>D2-H</sub>**, by adding OMe donor groups and CMe<sub>2</sub> bridges decreases  $J/k$  from 165 K down to 42 K. All these electron donor groups increase the induced electronic density at the level of the spin bearers, thus stabilizing them upon oxidation, but also at the level of the spin couplers, thus most probably exalting the antiferromagnetic sub-component of  $J$  ( $=J_F+J_{AF}$ ).

## Chemical structures of PB2 and PB3.



## X. References

- [1] K. Sonogashira, Y. Tohda, N. Hagihara, *Tetrahedron Lett.* **1975**, *16*, 4467-4470.
- [2] G. R. Fulmer, A. J. Miller, N. H. M.; Sherden, H. E. Gottlieb, A. Nudelman, B. M. Stoltz, J. E. Bercaw, K. I. Goldberg, *Organometallics* **2010**, *29*, 2176-2179.
- [3] CrysAlisPro, Oxford Diffraction Ltd., Version 1.171.36.24, **2012**.
- [4] G. M. Sheldrick, *Acta Cryst.* **2015** *A71*, 3-8.
- [5] O. V. Dolomanov, L. J. Bourhis, R. J. Gildea, J. A. K. Howard, H. J. Puschmann, *Appl. Cryst.* **2009**, *42*, 339-341.
- [6] S. Stoll, G. Jeschke, M. Willer and A. Schweiger, *Journal of Magnetic Resonance*, **1998**, *130*, 86-96.
- [7] A. Schweiger and G. Jeschke, *Principles of Pulsed Electron Paramagnetic Resonance*, Oxford University Press, Oxford, **2001**.

[8] (a) J. A. Gaj, R. Planel, G. Fishman, *Solid State Commun.* **1979**, *29*, 435-438; (b) J.A. Gaj, *Acta Physica Polonica*, 1988, **A73** 463, (c) A. Rajca, A. Olankitwanit, Y. Wang, P.J. Boratyński, M. Pink, S. Rajca, *J. Am. Chem. Soc.*, 2013, **135**, 18205-18215; (d) A. Rajca, A. Olankitwanit, S. Rajca, *J. Am. Chem. Soc.*, 2011, **133**, 4750-4753.

[9] O. Kahn, *Molecular magnetism*, VCH Publishers Inc., New York, 1993.

[10] J.B. Gosk, V. Maurel, S. Gambarelli, D. Djurado, R. Szymczak, A. Twardowski, I. Kulszewicz-Bajer *J. Appl. Phys.*, **2011**, *109*, 074911-6.

[11] Velde, G. T.; Baerends, E. J.; Numerical integration of polyatomic systems, *J. Comput. Phys.* **1992**, *99*, 84.

[12] Vosko, S. H.; Wilk, L.; Nusair, M. *Can. J. Phys.* **1980**, *58*, 1200.

[13] A. D. Becke, *Phys. Rev.* **1988**, *A38*, 3098-3100.

[14] J. P. Perdew, *Phys. Rev.* **1986**, *B33*, 8822-8824.

[15] G. T. Velde, E. J. Baerends, Numerical Integration for Polyatomic Systems. *J. Comput. Phys.* **1992**, *99*, 84-98.

[16] A. D. Becke, A New Mixing of Hartree-Fock and Local Density Functional Theories. *J. Chem. Phys.* **1993**, *98*, 1372-1377.

[17] L. Noodleman, *J. Chem. Phys.* **1981**, *74*, 5737;

[18] J. G. Norman, P. B. Jr.; Ryan, L. Noodlema, E. R. Davidson, *Chem. Phys.* **1986**, *109*, 131-143;

[19] L. Noodleman, C. Y. Peng, D. A. Case, J. -M. Mouesca, *Coord. Chem. Rev.* **1995**, *144*, 199-244.

[20] L. Noodleman, C.Y. Peng, D.A Case, J.-M. Mouesca, *Coord. Chem. Rev.* **1995**, *144*, 199-244.